

Cranfield

College of Aeronautics Report No. 9009
May 1990



Measurement of the Longitudinal Static Stability and the
Moments of Inertia of a 1/12th Scale Model of a B.Ae Hawk

H A Hinds & M V Cook

Sixth Quarterly Report
May 1990

College of Aeronautics
Cranfield Institute of Technology
Cranfield, Bedford MK43 0AL, England



1401594816

Cranfield

College of Aeronautics Report No. 9009
May 1990



Measurement of the Longitudinal Static Stability and the
Moments of Inertia of a 1/12th Scale Model of a B.Ae Hawk

H A Hinds & M V Cook

Sixth Quarterly Report
May 1990

College of Aeronautics
Cranfield Institute of Technology
Cranfield, Bedford MK43 OAL, England

ISBN 1 871564 07 7

£8.00

*"The views expressed herein are those of the authors alone and do not
necessarily represent those of the Institute"*

ACKNOWLEDGEMENTS

The research which is the subject of this report was initiated by MOD(PE), Aerodynamics Dept., Royal Aerospace Establishment, Farnborough, in response to a proposal by the College of Aeronautics under the terms of Agreement No.2082/192.

The support and encouragement of the technical monitor, Dr. A.J. Ross is gratefully acknowledged.

"The views expressed herein are those of the authors alone and do not necessarily represent those of the Institute"

<u>CONTENTS</u>	<u>PAGE</u>
1.0 INTRODUCTION	4
2.0 LONGITUDINAL STABILITY EVALUATION	5
2.1 HAWK GEOMETRY AND THEORY	6
2.2 EXPERIMENTAL PROCEDURE	8
2.3 CALIBRATION OF BALANCE	11
2.4 DERIVATION OF C_L, C_D, C_M	13
2.5 EXPERIMENTAL ERROR	14
3.0 ANALYSIS OF LONGITUDINAL STATIC STABILITY DATA	15
3.1 MEAN DOWNWASH AT TAILPLANE	16
3.2 TAILPLANE LIFT CURVE SLOPE	18
3.3 LOCATION OF AERODYNAMIC CENTRE (A.C.) FOR THE TAILLESS AIRCRAFT	20
3.4 THE STATIC MARGIN (STICK FIXED)	21
3.5 FURTHER CONFIRMATION OF THE VALUE OF h_n	23
3.6 DISCUSSION	24
4.0 AIRCRAFT/MODEL SCALING LAWS	27
4.1 SUMMARY OF SIMILARITY LAWS	31
4.2 SCALING OF DERIVATIVES	32
4.2.1 NON-DIMENSIONAL MASS AND INERTIA	32
4.2.2 CONCISE LONGITUDINAL DERIVATIVES	33
4.2.3 CONCISE LATERAL DERIVATIVES	34
5.0 MEASUREMENT OF MOMENTS OF INERTIA	35
5.1 PITCH INERTIA	39
5.2 ROLL INERTIA	41
5.3 YAW INERTIA	42
6.0 DATA ACQUISITION SYSTEM	43
7.0 CONCLUSION	44
REFERENCES	45
APPENDIX A: C_M vs C_L GRAPHS AT DIFFERENT REFERENCE POINTS	
APPENDIX B: PITCH AND ROLL OSCILLATION DECAY GRAPHS	
APPENDIX C: PROGRAM FOR DATA CONVERSION AND DIFFERENTIATION	

<u>LIST OF FIGURES</u>		<u>PAGE</u>
FIG. 1	HAWK GEOMETRY (PLAN VIEW)	7
FIG. 2	HAWK ON TEM BALANCE, TAIL-ON	10
FIG. 3	HAWK ON TEM BALANCE, TAIL-OFF	10
FIG. 4	LIFT FORCE CALIBRATION	12
FIG. 5	DRAG FORCE CALIBRATION	12
FIG. 6	PITCHING MOMENT CALIBRATION	12
FIG. 7	TAILPLANE ANGLE OF INCIDENCE AND DOWNWASH	16
FIG. 8	C_{M_p} vs α CURVES (TAIL-ON AND TAIL-OFF)	17
FIG. 9	MEAN DOWNWASH ANGLE vs ANGLE OF INCIDENCE	17
FIG. 10	TAILPLANE LIFT CURVE SLOPE	19
FIG. 11	WHOLE AIRCRAFT LIFT CURVE SLOPE	19
FIG. 12	C_{M_p} vs C_L TAIL-OFF	21
FIG. 13	C_{M_p} vs C_L (TAIL-ON FOR VARIOUS η)	23
FIG. 14	C_M vs C_L ($\eta=0$, VARIOUS POSITIONS)	26
FIG. 15	SUMMARY OF IMPORTANT POSITIONS ON THE HAWK MODEL	26

1.0 INTRODUCTION.

A programme of research sponsored by the Royal Aerospace Establishment at Farnborough is currently in progress in the College of Aeronautics at Cranfield Institute of Technology. The programme is to investigate the use of a Modified Stepwise Regression (MSR) procedure to estimate the stability and control parameters of a small B.Ae. Hawk aircraft model flown in a dynamic wind tunnel facility at Cranfield. Details of the MSR procedure are given in References 1 and 2. This report will present the work carried out during the past three months on the Hawk model and the dynamic rig facility.

One aim of the last quarter was to gain familiarisation with the dynamic rig, Hawk model and electronic control unit. This was achieved through the work for the measurement of the model moments of inertia, which is presented in section 5.0.

Another aim of this quarter was to sort out the longitudinal stability of the model as it has previously been difficult to control and trim when flown in the wind tunnel. That the model was difficult to control is surprising as the full scale B.Ae Hawk is a stable aircraft and a correctly scaled model should also be stable. The reason for this discrepancy was thought to be due to the gimbal pivot being positioned too far aft in the model. This has been demonstrated experimentally and details of the analysis of the longitudinal static stability of the model are presented in sections 2.0 and 3.0.

Section 4.0 presents a summary review of various scaling laws and gives details of some full scale Hawk and model Hawk parameters.

A BASIC program to convert recorded data to the ASCII format required by the MSR program has been written. Also included in this program is a numerical method to generate attitude angle rate data by the numerical differentiation of specified channels. Section 6.0 describes the progress made with the data acquisition system.

2.0 LONGITUDINAL STATIC STABILITY EVALUATION.

As mentioned, the Hawk model is difficult to trim when flown in the wind tunnel. Attempts to secure stability of the model by moving the c.g. forward does not help the situation in any way and only changes the tailplane angle required to trim. So experiments have been undertaken to assess longitudinal static stability characteristics of the model. The experimental objectives were:

1. To estimate the variation of mean downwash angle at the tailplane with incidence.
2. To estimate the tailplane lift curve slope.
3. To estimate the location of the aerodynamic centre for the wing and body only.
4. To derive the lift trim curve of the model aircraft.
5. To predict the stick fixed static c.g. margin.

The experiments also provided an opportunity to obtain some aerodynamic data from which other useful information could be derived, such as stability derivative estimates.

SOME DEFINITIONS:

h_0 : is the position of the aerodynamic centre (A.C.) of the aircraft minus the tailplane, which is shifted forwards of the aerodynamic centre of the wing alone by the presence of the fuselage

h_n : is the position of the neutral point (N.P.) which is the aerodynamic centre of pressure of the complete aircraft with tailplane attached and controls fixed.

C.G. RANGE: The centre of gravity of an aircraft has forward and aft limits set by diminishing ability to trim by means of control surface deflection (forward limit) and diminishing stability (aft limit). The c.g. range and limits are usually expressed in terms of a percentage of the standard mean chord (SMC) \bar{c} .

STATIC MARGIN ($K_n = h_n - h$): This is the distance measured as a fraction of the SMC between the c.g. and the neutral point. In the absence of aeroelastic distortion and compressibility effects, the static margin is equal to the c.g. margin.

2.1 HAWK GEOMETRY AND THEORY.

The Hawk model reference line is taken as the leading edge of the wing where it intercepts the fuselage. For convenience, the location \bar{c} has been moved forward to be coincident with the distance aft from the leading edge reference line. Figure 1 shows this position and defines various points on along the chord line aft of this reference line.

The position of the c.g. is in front of the TEM pivot and has been arranged to coincide with the position of the gimbal centre inside the model fuselage.

When experimental readings of the pitching moment are taken they are related to the position h_p of the pivot point of the model on the TEM Balance. Therefore, taking moments about the TEM BALANCE pivot point leads to the following expression:

$$M_p = M_o + L_{WB}(h_p - h_o)\bar{c} - mg(h_p - h)\bar{c} - L_T\{l_t - (h_p - h)\bar{c}\} \quad \text{EQN. (1)}$$

\uparrow \uparrow \uparrow \uparrow
 const wing/body const tail contribution

For trim: $M_p = 0$ must be true and this will give the tailplane angle η required to trim the aircraft.

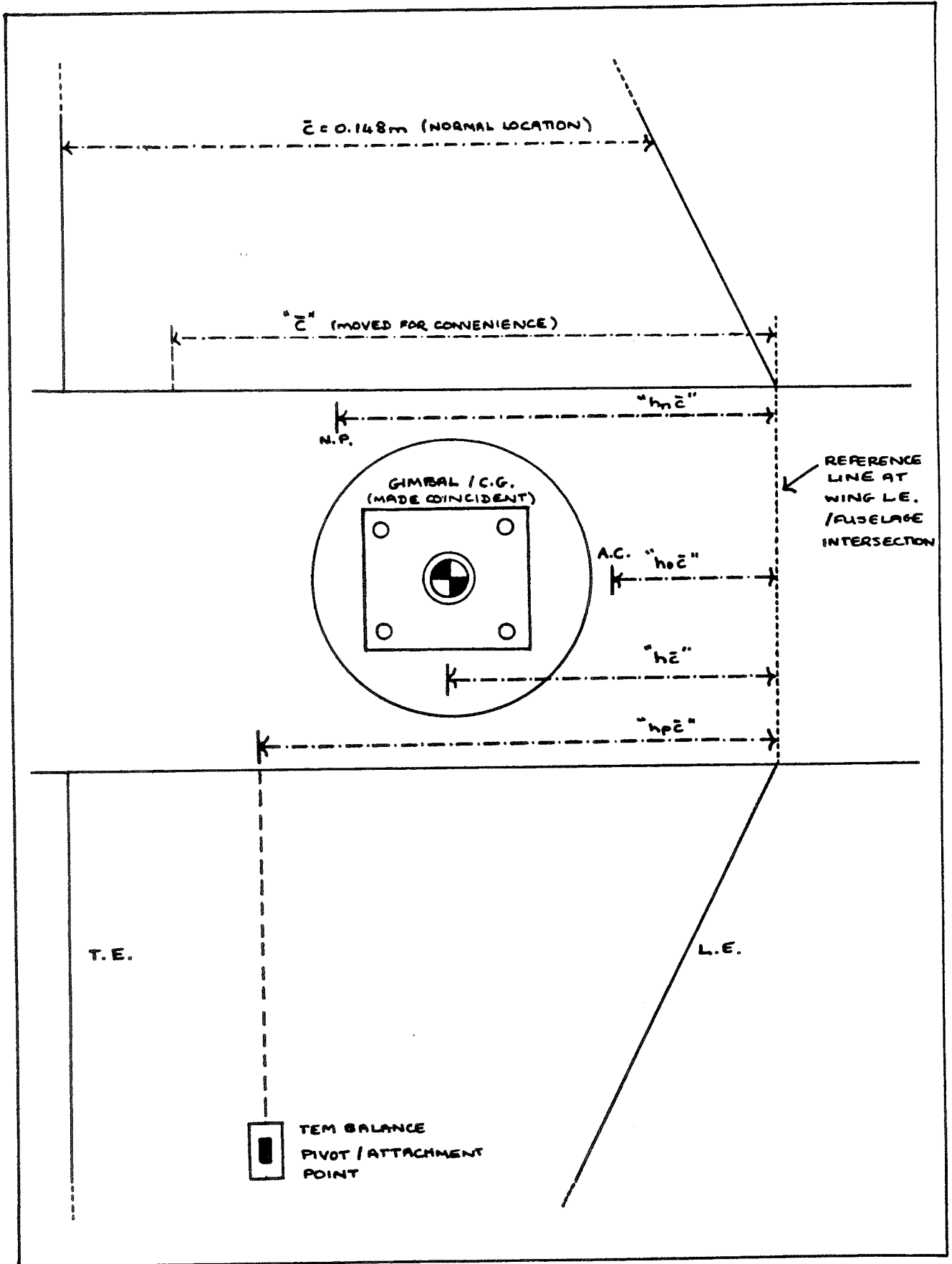
For stability about "p": $dM_p/dC_L < 0$ is required. From Eqn. 1 this would imply that the stability is not influenced by M_o or the term $mg(h_p - h)$. Therefore the c.g. position only influences the angle to trim and it is the position of the TEM pivot which is important. A stable trim of the aircraft can only be achieved if the pivot point on the TEM is ahead of the neutral point of the model.

$$\text{For the tailless aircraft } dC_{M_p} / dC_L = h_o - h \quad \text{EQN. (2)}$$

$$\text{and for the whole aircraft } dC_{M_p} / dC_L = h_p - h_n \quad \text{EQN. (3)}$$

Thus from the experimental results knowing dC_{M_p} / dC_L and the TEM reference point h_p , it should be possible to calculate h_o and h_n .

FIG 1: HAWK GEOMETRY (PLAN VIEW).



2.2 EXPERIMENTAL PROCEDURE.

The Hawk model was mounted on a TEM three component force and moment balance in the open test section of the Weybridge low speed wind tunnel. There were three mounting points on the model, these consisting of two struts, one on each wing and one strut on the rear fuselage. The position of the two wing struts will be referred to as the "TEM PIVOT POINT". The load ranges of the balance are given below:

<u>COMPONENT</u>	<u>LOAD RANGE</u>	<u>ACCURACY</u>
Lift	0-10 Kg	25 gm
Drag	0-3.5 Kg	10 gm
Pitch Moment	0-175 gm.m	1.75 gm.m
Incidence Range	-10 to 40°	

The following procedure was carried out with the tail-on: (FIG.2)

1. The ambient temperature and pressure were recorded.
2. The Hawk model was set up at an initial indicated incidence of -4 degrees.
3. The wind off lift (L), drag (D) and pitching moment (P) outputs were recorded in volts.
4. The wind tunnel speed was set to give a nominal 60 to 70 mm H₂O on the Betz manometer.
5. The tailplane was set to angles of -5,0,2,5 and 10 degrees and the values of L, D and P recorded for each tailplane setting.
6. The tunnel was stopped and the wind off values of L, D and P recorded again.
7. Steps 3-6 were repeated for a range of incidences from -2 to 14°
8. Further, at model incidences of 2 and 4 degrees values of L, D and P were taken for a number of tailplane setting angles which ranged from -14 to +14 degrees in 2 degree steps.

The following procedure was carried out with the tail-off: (FIG.3)

1. For the range of incidences from -4 to +14 degrees L, D and P were recorded for a nominal speed between 60 and 70 mm H₂O.
2. The wind off values of L, D and P were recorded before and after each tunnel run for a particular incidence.

Finally, the tare drag correction was estimated for no model on the balance and piano wire connected between each strut support. A calibration of the balance was carried out as described in § 2.3.

FIG. 2: HAWK ON TEM BALANCE, TAIL-ON.

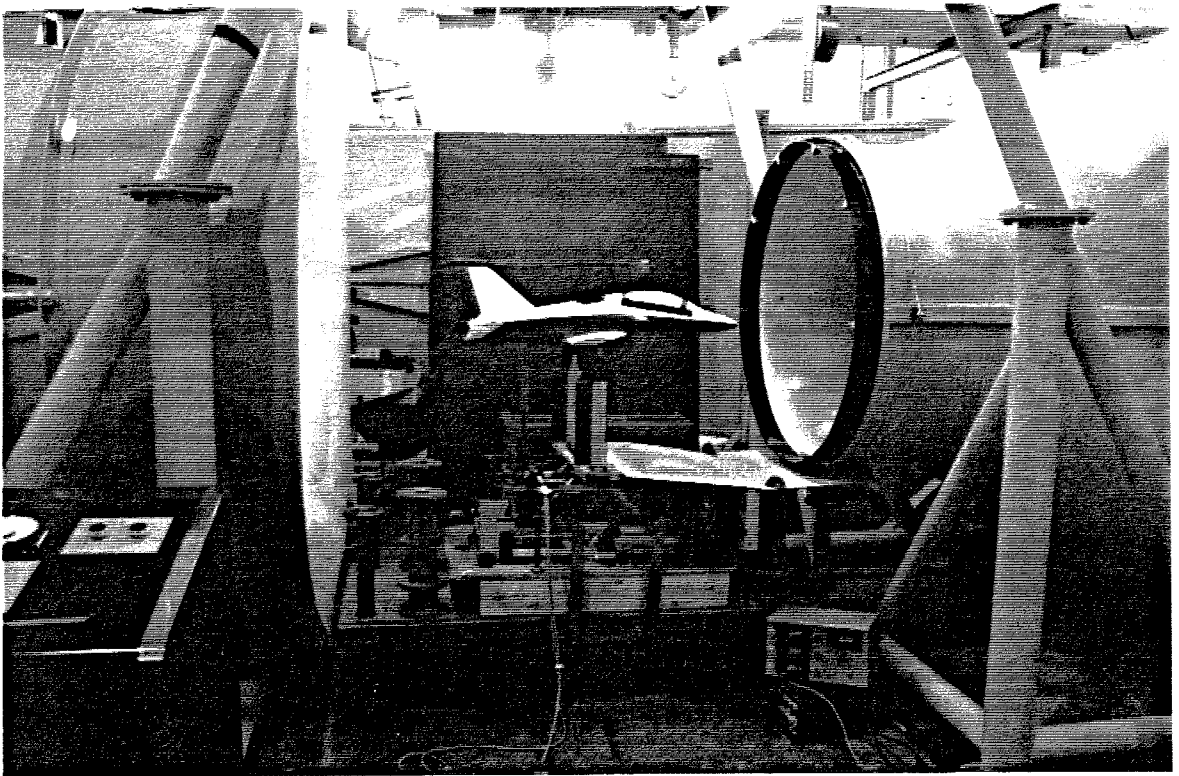
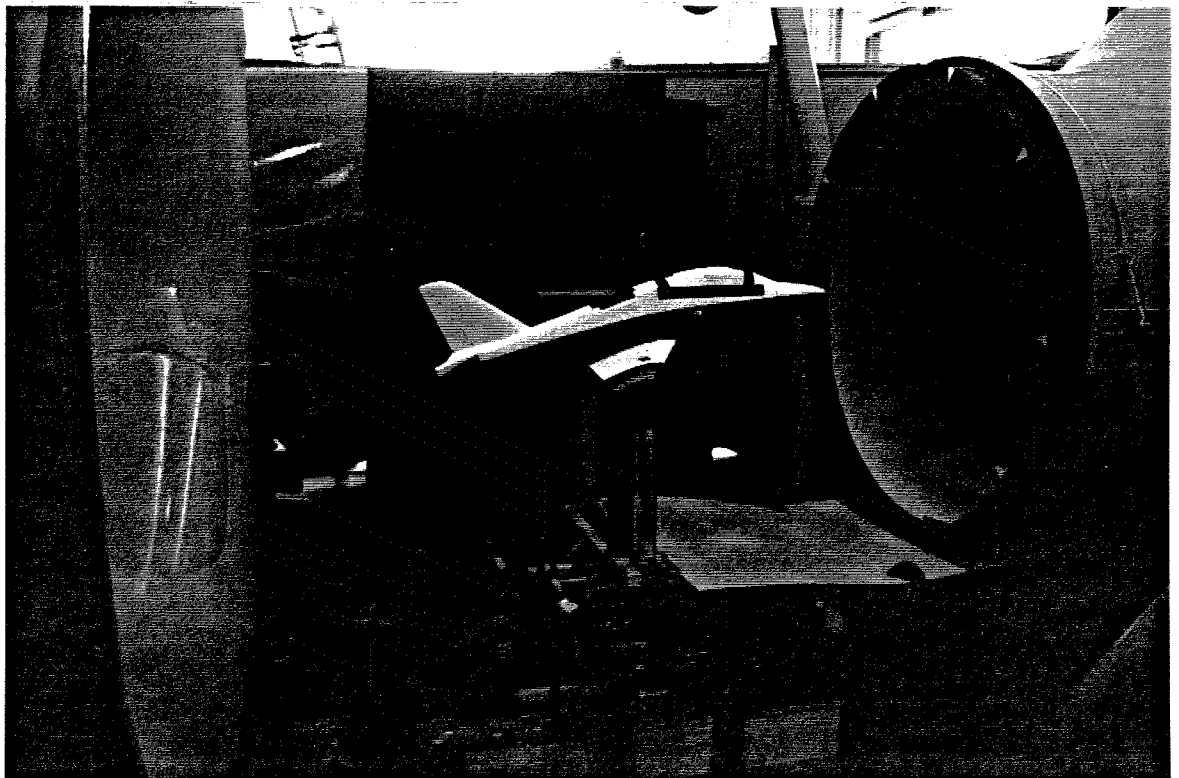


FIG. 3: HAWK ON TEM BALANCE, TAIL-OFF.



2.3 CALIBRATION OF THE BALANCE.

Wind off values of the L, D and P outputs were taken both before and after each wind tunnel run as these figures tended to vary quite considerably. If the balance was left for a few minutes after running the tunnel it would appear that the power supply and transducers of the balance would warm up and change the wind off outputs. To improve this situation the whole balance was lowered to try and reduce the proportion of the balance in the wind stream. Also, a large plywood was fairing placed in front of the power supply to minimise the cooling effect of the tunnel air stream. These measures led to better before and after wind off output figures. It was decided to take wind off values of the outputs as soon as the air flow stopped after switching off the wind tunnel as these should be closest to the actual "zero" outputs of the balance when readings are taken with the wind on.

To calibrate the TEM balance the model was removed and a special "T-shaped" bar attached to the balance struts. Known weights were then hung from the balance using fishing wire and the appropriate output voltages recorded.

For LIFT:

Weights were hung midway along the bar connecting the two wing struts to give a negative lift force. Fig. 4 shows the calibration line obtained. This has a slope of -213.48 N/V.

For DRAG:

Fishing line was run horizontally from the bar between the wing struts and over a pulley at the rear of the balance. The voltages obtained for various weights hung from the rear of the apparatus to simulate the drag force were recorded. Fig. 5 shows the drag calibration line which has a slope of -83.56 N/V.

For PITCHING MOMENT:

To produce a positive pitch up moment for the balance, weights were hung 5 cm back along the T-bar from the wing strut connection bar. The appropriate voltages were recorded and the corresponding pitching moment calculated. Fig. 6 shows the calibration line obtained and this has a slope of 7.39 Nm/V.

FIG.4: LIFT FORCE CALIBRATION

$dY/dX = -213.48 \text{ N/V}$

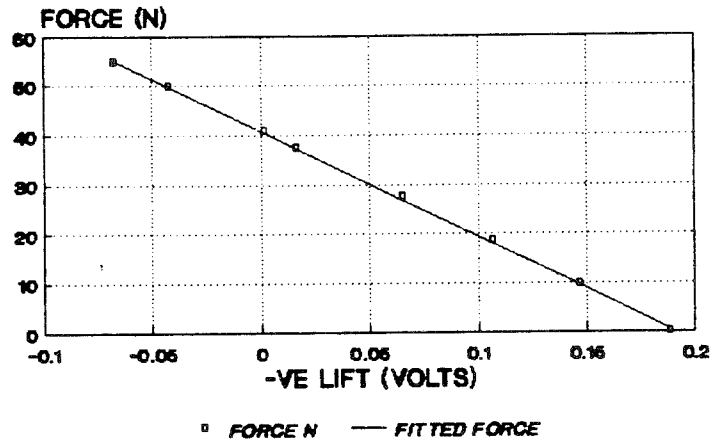


FIG.5: DRAG FORCE CALIBRATION

$dY/dX = -83.56 \text{ N/V}$

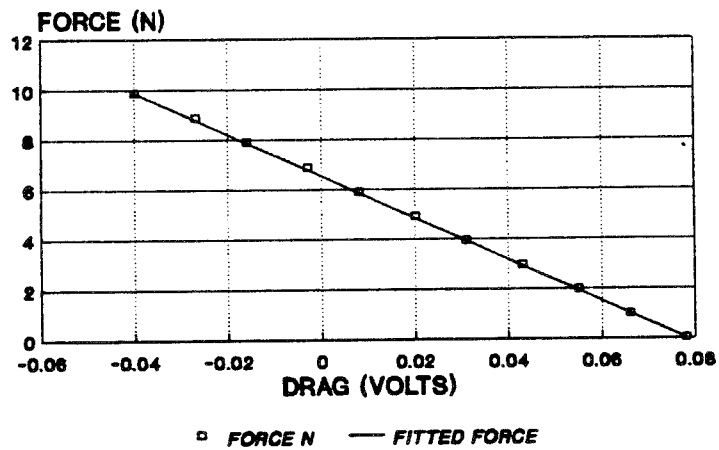
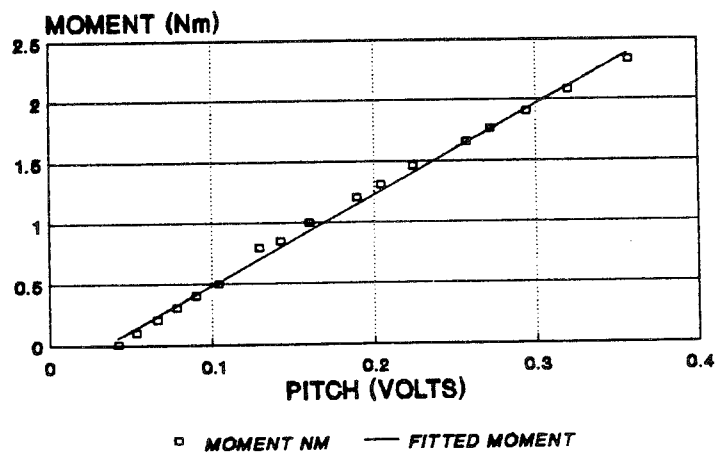


FIG.6: PITCHING MOMENT CALIBRATION.

$dY/dX = 7.39 \text{ Nm/V}$



2.4 DERIVATION OF C_L , C_D AND C_M .

A BASIC program exists in the College of Aeronautics for the analysis of data from a similar experiment using a 1/22.5 th scale model of the D.H. Dove 104 mounted on the TEM balance. The BASIC program was suitably changed to include the relevant Hawk model data (given in § 3.0) and the new TEM balance calibration figures obtained from the previous section. The program was also changed to allow the tailplane angle to be entered and output as well as just the normal incidence angle. Further changes allowed a balance wind off zero output voltage to be entered for every reading taken instead of the wind off output being assumed constant throughout the experiment. The program carries out the following operations to the balance voltage data in order to calculate the lift, drag and pitching moment coefficients:

1. Each reading is corrected for the zero wind off balance output.
2. The drag tare correction is taken away from each drag voltage.
3. The voltages are converted to lift (L) and drag (D) force in Newtons and pitching moment (M) in Newton-metres.
4. The betz manometer reading is converted from mm H₂O to the wind tunnel speed as shown below.
5. The non-dimensional lift, drag and pitching moment coefficients are calculated with reference to the TEM pivot point using:

$$C_L = L/0.5\rho V^2 S; \quad C_D = D/0.5\rho V^2 S; \quad C_M = M/0.5\rho V^2 S \bar{c} \quad \text{EQNS. (4)}$$

A later change to the program was also made to enable the calculation of C_m at different positions on the model.

CONVERSION FROM $h = \text{mm H}_2\text{O}$ (BETZ) TO WIND TUNNEL SPEED V (m/s).

Dynamic pressure: $q = 0.5\rho_0 V^2$ $\rho_0 = \text{S.L. air density} = 1.225 \text{ kg/m}^3$

Weybridge pressure calibration: $\Delta P_{\text{betz}} = 1.015.q$

Also $\Delta P_{\text{betz}} = \rho g h$

$\rho = \text{water density} = 1000 \text{ kg/m}^3$

$g = \text{gravitational acceln.} = 9.81 \text{ m/s}^2$

Hence

$$V^2 = \frac{2\rho g h}{1.015\rho_0} = \frac{(h \times 10^{-3}) \cdot (2) \cdot (1000) \cdot (9.81)}{(1.015) \cdot (1.225)} = h \times 15.78 \quad \text{EQN. (5)}$$

2.5 EXPERIMENTAL ERROR.

Since the Weybridge tunnel is an open jet facility, the dynamic pressure correction can be assumed to be negligible. The other corrections which should be applied are as follows:

$$(i) \quad \alpha_{\text{true}} = \alpha_{\text{measured}} + \delta\alpha \quad \text{EQN.(6)}$$

where the incidence correction, $\delta\alpha$ is given by:

$$\delta\alpha = \sigma.(S/C).C_L \quad \begin{array}{l} C = \text{cross sectional area of wind tunnel} \\ S = \text{wing area} \\ \sigma = \text{mean wing interference factor} \end{array}$$

$$(ii) \quad C_{D_{\text{true}}} = C_{D_{\text{measured}}} + \sigma.(S/C).C_L^2 \quad \text{EQN.(7)}$$

However, at present the value of σ is not known and so all the values of measured incidence α and the drag coefficient C_D will be slightly wrong in this report. It is planned to calculate the value for σ and to re-present this work in a later report on the MSR programme in the near future.

A second cause of experimental error is due to the fact that the outputs of the TEM balance did not always have the same before and after "wind off" readings. Unfortunately the pitch output varied the most and often sets of experiments were repeated to try and minimise the difference in output and check for repeatability of readings.

3.0. ANALYSIS OF LONGITUDINAL STATIC STABILITY DATA.

There are a number of basic assumptions made for the analysis techniques to be used later in this section. These assumptions are approximately true only for the case of an aircraft in a power-off low speed glide and are as follows:

1. The aircraft structure is completely rigid.
2. Compressibility effects are negligible.
3. The non-dimensional lift, drag and pitching moment coefficients are independent of forward speed.
4. There is no vertical displacement of the C.G. from the wing chord line.
5. Tailplane lift is small in comparison with wing lift and the movement of the tailplane centre of pressure is negligible.
6. The flight path is approximately horizontal.

RELEVANT FIXED MODEL AIRCRAFT DATA

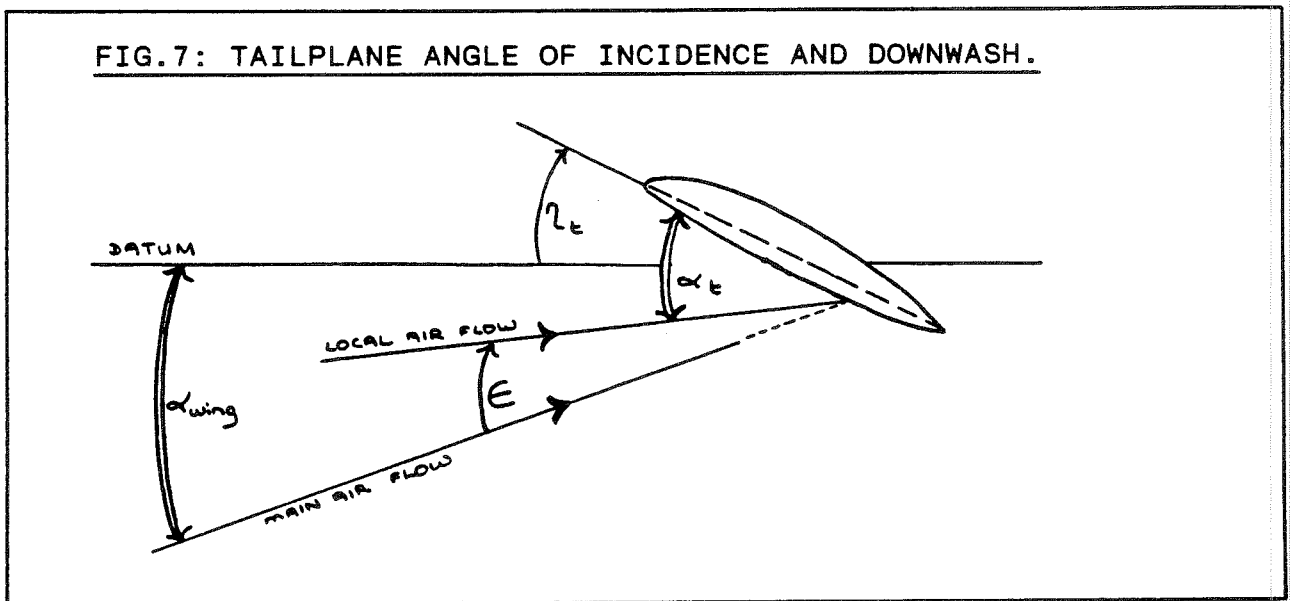
Gross wing area (S)	= 0.115 m ²
Root chord	= 0.221 m
Tip chord	= 0.075 m
Wing span	= 0.782 m
Mean geometric chord (\bar{c})	= 0.148 m
Tailplane gross area (S _T)	= 0.029 m ²
Tailplane moment arm (l _T)	= 0.358 m
Reference line = point of intersection of wing l.e. and fuselage.	
TEM pivot point (h _p) = 0.797 \bar{c} = 118 mm aft of reference line.	
Centre of gravity (h) = 0.686 \bar{c} = 101.5 mm aft of reference line.	

WEYBRIDGE TUNNEL DATA

Jet diameter	= 42" = 1.067 m
Length of jet	= 60" = 1.524 m
Collector diameter	= 50" = 1.270 m
Fan diameter	= 48" = 1.219 m
Maximum contraction ratio	= 4.4
Maximum H.P. of fan motor	= 35
Maximum tunnel speed	= 130 ft/sec = 39.6 m/s

3.1 MEAN DOWNWASH AT TAILPLANE.

The effective angle of incidence of the tailplane is determined by the degree of downwash generated by the main wing. In order to estimate this mean downwash a comparison is made between C_{M_p} at various tailplane angles and C_{M_p} for the wing and body alone. Fig.7 ,below, depicts what is meant by the downwash angle ϵ and shows the tailplane angle of incidence α_t :



$$\alpha_t = \alpha_w + \eta - \epsilon \quad \text{EQN.(8)}$$

A graph of C_{M_p} vs α_w was plotted for each tailplane angle α_t . On the same graph (Fig.8), C_{M_p} vs α_w was plotted for the tail-off configuration. Points of intersection of the tail on and tail-off graphs correspond to angles of zero tailplane lift. Therefore, if the tailplane is a symmetrical section, it is aligned to the local flow angle (ie. $\alpha_t = 0$) and thus gives a measure of the downwash. For each value of α_w , the points of intersection of the curves were estimated from Fig.8 and the downwash angle estimated using:

$$\epsilon = \alpha_w + \eta \quad \text{EQN.(9)}$$

A plot of ϵ vs α_w was then made, Fig.9. Assuming a linear relationship, the rate of change of mean downwash angle with incidence was calculated and found to be:

$$\underline{d\epsilon/d\alpha_t = 0.57}$$

FIG. 8: C_{mp} vs α CURVES (TAIL-ON AND TAIL-OFF).

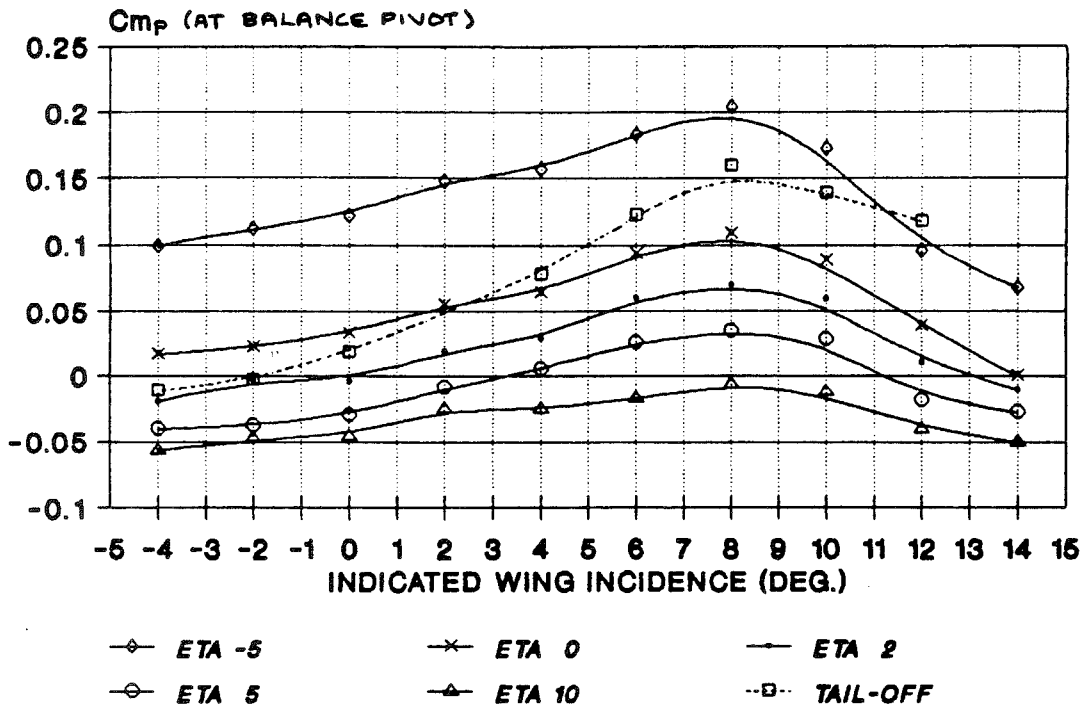
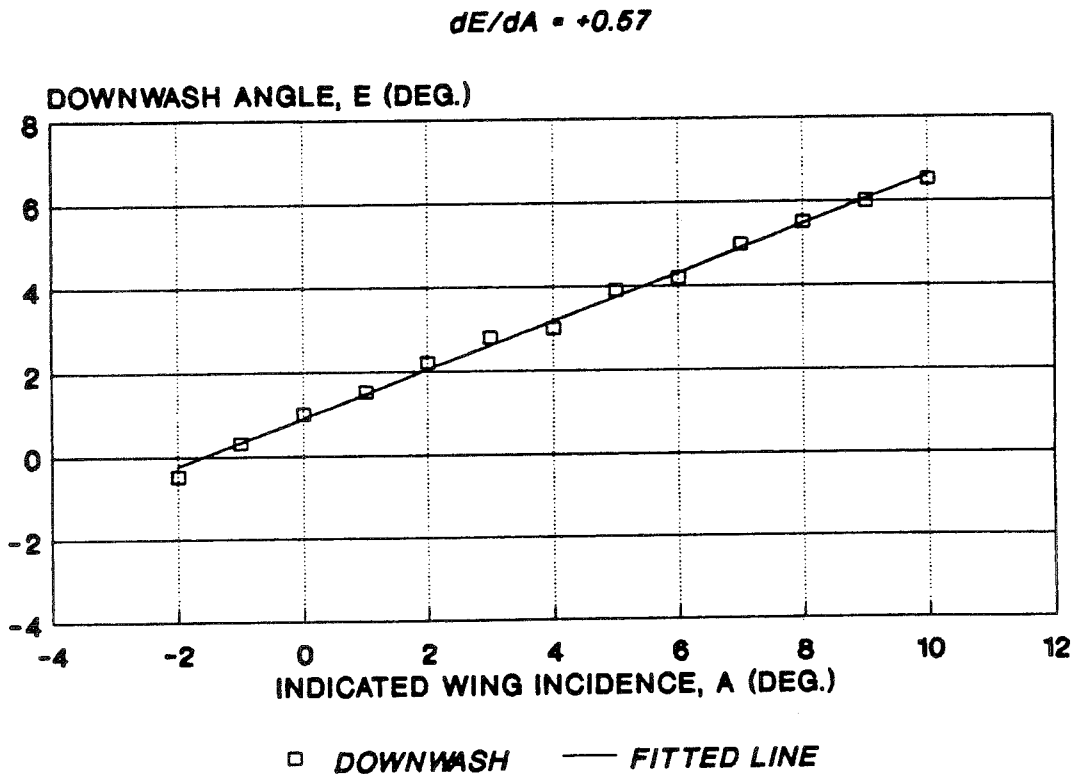


FIG. 9: MEAN DOWNWASH ANGLE vs ANGLE OF INCIDENCE.



3.2 TAILPLANE LIFT CURVE SLOPE.

The tailplane lift curve slope is usually evaluated from the C_M vs. α data at a specified incidence. The difference in pitching moment (δC_M), between tail-off and tail-on aircraft configurations at the given incidence (α) and tailplane angle (η_t) corresponds to the moment due to the tailplane lift C_{L_t} about the balance pivot point. It is therefore possible to convert values of δC_M to C_{L_t} knowing the tailplane moment arm (α_t), the tailplane area (S_t), the wing area (S) and the geometric mean chord (\bar{c}).

It was decided to use an incidence angle of $\alpha = 4^\circ$, being at the middle of the aircraft trim range. Values of C_M (tail-on) and C_M (tail-off) were tabulated for each tailplane angle (η_t). The pitching moment, (C_{M_t}), due to the tailplane was calculated using:

$$C_{M_t} = C_M (\text{tail-on}) - C_M (\text{tail-off}) \quad \text{EQN. (10)}$$

Next, the pitching moment due to the tailplane was converted into a tailplane lift coefficient (for each value of η_t) using the relation:

$$-C_{L_t} \bar{V} = C_{M_t} \quad \text{EQN. (11)}$$

where the tailplane volume coefficient $\bar{V} = \frac{l_s S_t}{l \bar{c}} = 0.61$

From Fig.9, the downwash angle for $\alpha = 4$ is estimated to be $\epsilon = 3.2$. Thus the tailplane incidence angle α_t may be corrected using Eqn. 8 as follows:

$$\begin{aligned} \alpha_t &= \alpha_w + \eta - \epsilon \\ \rightarrow \alpha_t &= 4 + \eta - 3.2 \end{aligned}$$

A plot of α_t vs C_{L_t} was then made and is shown in Fig.10. From this the tailplane lift curve slope was estimated from a linear portion of the slope; it was found to be:

$$\underline{a_1 = dC_{L_t} / d\alpha_t = 0.04 \text{ deg}^{-1} \text{ or } 2.3 \text{ rad}^{-1}}$$

The lift curve graph for the whole aircraft (tail and wing) is also shown over leaf, in Figure 11 and this has a slope of:

$$\underline{a = dC_L / d\alpha = 0.065 \text{ deg}^{-1} \text{ or } 3.7 \text{ rad}^{-1}}$$

FIG. 10: TAILPLANE LIFT CURVE SLOPE.

$A_1 : dCL(\text{tail})/dA(\text{tail}) : 0.04 \text{ (DEG}^{-1}\text{)}$

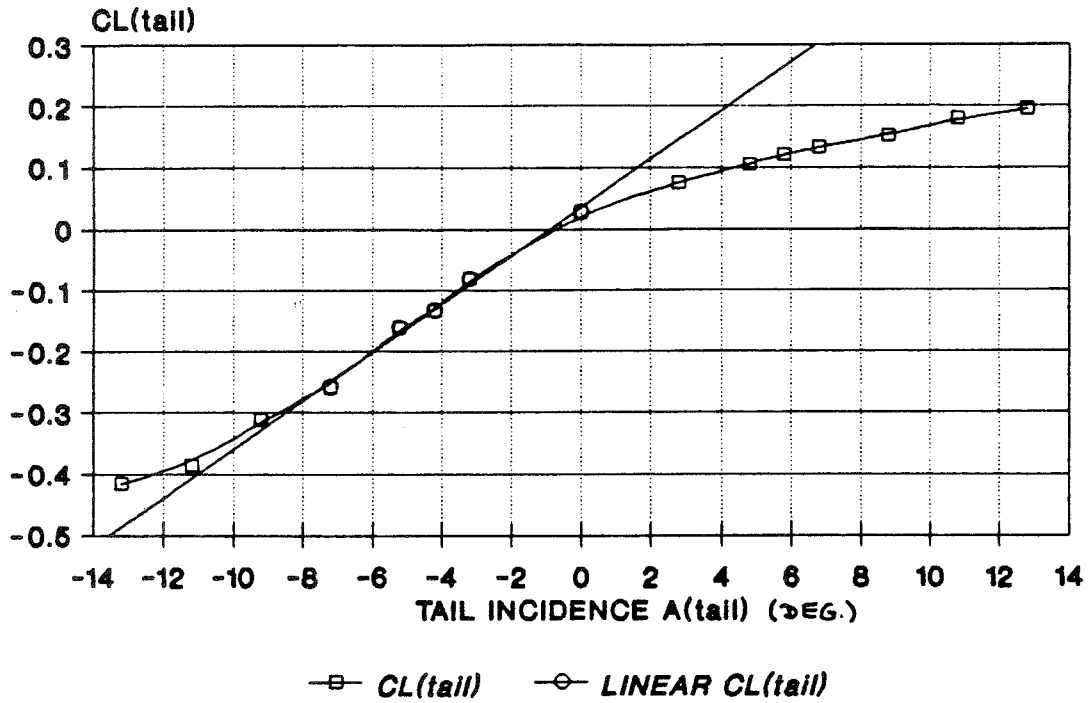
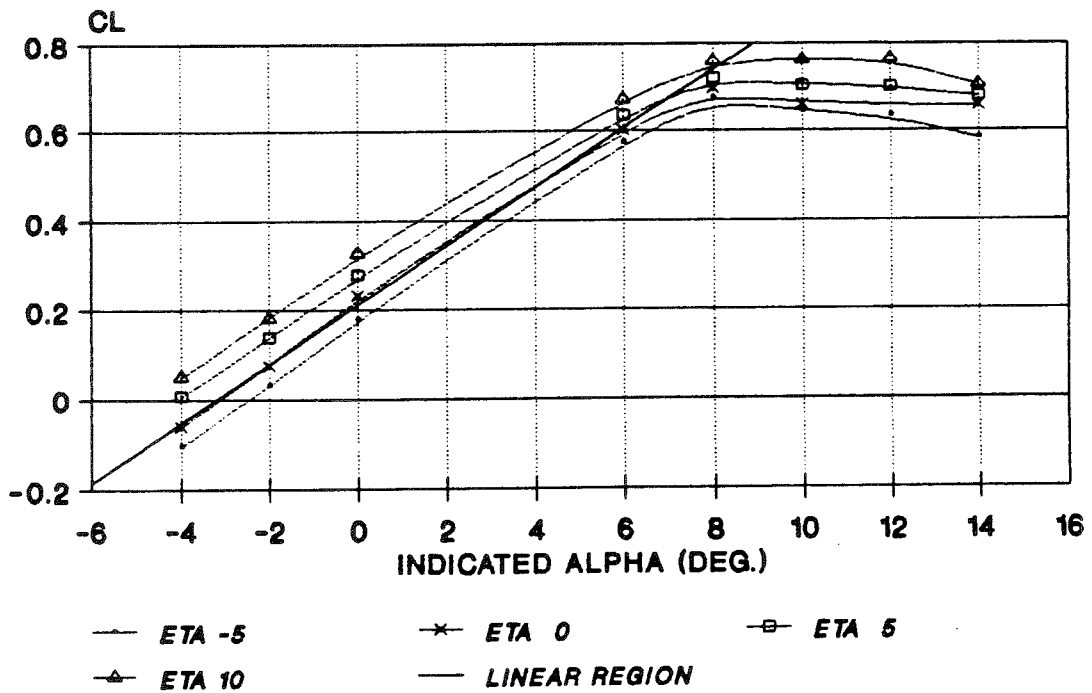


FIG. 11: WHOLE AIRCRAFT LIFT CURVE SLOPE.

$A : dCL/dA : 0.065 \text{ (DEG}^{-1}\text{)}$



3.3 LOCATION OF THE AERODYNAMIC CENTRE FOR THE TAILLESS AIRCRAFT.

The pitching moment equation of Eqn. 1 may also be written in the following form:

$$C_{M_p} = C_{M_o} + C_L(h_p - h_o) - \bar{V}[a_1(\alpha + \eta_t - \bar{\epsilon}) + a_2\eta] \quad \text{EQN. (11)}$$

\uparrow const \uparrow wing/body \uparrow tail moment

where

$$a_1 = dC_{L_t}/d\alpha_t \quad a_2 = dC_{L_t}/d\eta \quad a = dC_L/d\alpha$$

C_{M_o} = the pitching moment about the aerodynamic centre for the tailless aircraft.

h_p, h_o = non-dimensional distances of the balance pivot point and the aerodynamic centre aft of the reference line

Differentiating Eqn. 11 with respect to C_L , assuming C_{M_o} and η_t are constants and that the stick is fixed, gives:

$$\frac{dC_{M_p}}{dC_L} = (h_p - h_o) - \bar{V} \cdot a_1 \cdot \left(\frac{d\alpha}{dC_L} - \frac{d\epsilon}{dC_L} \right)$$

$$\frac{dC_{M_p}}{dC_L} = (h_p - h_o) - \bar{V} \frac{a_1}{a} \left(1 - \frac{d\epsilon}{d\alpha} \right) \quad \text{EQN. (12)}$$

For the tailless aircraft this equation becomes:

$$\boxed{\left(\frac{dC_{M_p}}{dC_L} \right)_{\text{tail-off}} = (h_p - h_o)} \quad \text{EQN. (13)}$$

A graph of C_{M_p} vs C_L for the tail-off configuration was plotted, as shown in Fig. 12. From this graph the gradient of the linear region of the graph was found to be

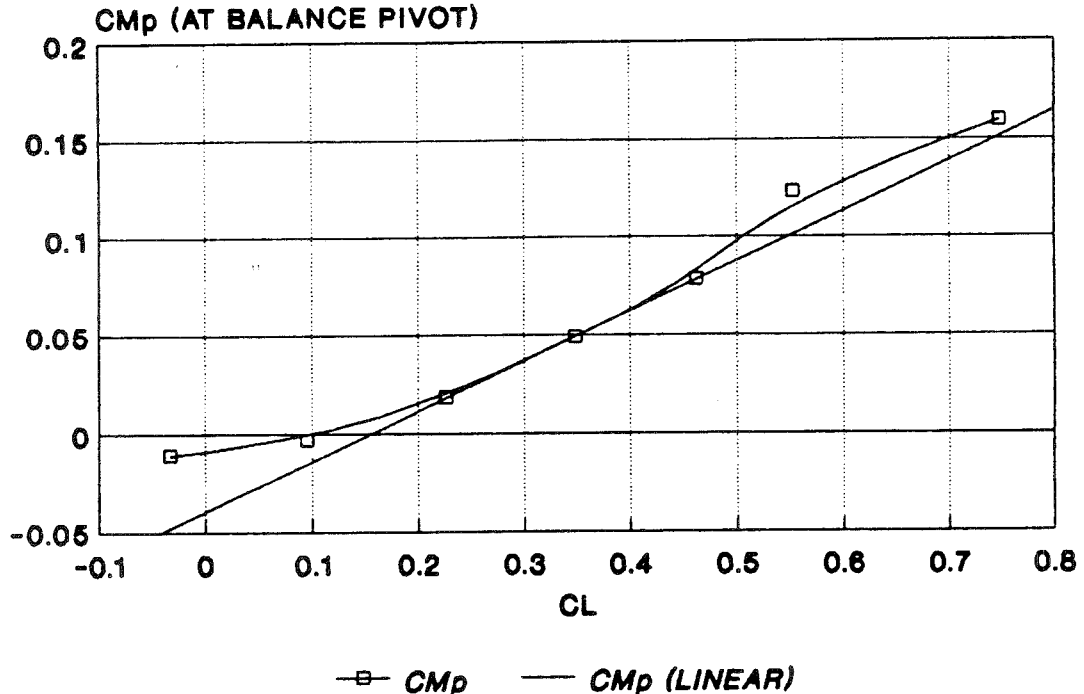
$$\left(\frac{dC_{M_p}}{dC_L} \right)_{\text{tail-off}} = 0.254$$

For the Hawk model $h_p = 0.797\bar{c}$. Thus the location of the aerodynamic centre (h_o) for the body and wing is:

$$\underline{h_o = 0.543\bar{c}} \quad \text{ie. } \underline{80.4 \text{ mm aft of the reference line.}}$$

FIG. 12: C_{M_p} vs C_L TAIL-OFF.

$$dC_{M_p}/dC_L : +0.254 : h_p - h_o$$



3.4 THE STATIC MARGIN (STICK FIXED).

. If the stick is fixed, the pitching moment equation can be written:

$$\left(\frac{-dC_{M_{cg}}}{dC_L} \right)_{\text{stick fixed}} = -(h - h_o) + \bar{V} \frac{a_1}{a} \left(1 - \frac{dc}{d\alpha} \right) \quad \text{EQN. (14)}$$

Note: the signs are usually changed in this way, since $(dC_{M_{cg}}/dC_L)$ must be negative to give positive static stability.

All the quantities in this equation are fixed by the aircraft configuration except h , the position of the c.g. By varying the value of h the stability can be made positive, negative or zero. Rearward movement of the c.g. increases $(h-h_o)$ and is therefore destabilising. The position of the c.g. which gives neutral stability is designated h_n and is called the *stick fixed neutral point*.

Substituting into the differential form of the pitching moment equation (Eqn.14) gives:

$$0 = -(h - h_0) + \bar{V} \frac{a_1}{a} \left(1 - \frac{d\epsilon}{d\alpha} \right)$$

$$\therefore \bar{V} \frac{a_1}{a} \left(1 - \frac{d\epsilon}{d\alpha} \right) = (h_n - h_0) \quad \text{EQN. (15)}$$

Substituting this tailplane term back into the original equation 14 gives an expression for the stability of the aircraft for any position of the c.g. as shown below:

$$\left(\frac{-dC_{M_{cg}}}{dC_L} \right)_{\text{stick fixed}} = -(h - h_0) + (h_n - h_0) = (h_n - h) \quad \text{EQN. (16)}$$

The distance of the c.g. from the stick fixed neutral point is called the *static centre of gravity margin, stick fixed* (H_n).

However, all of the experimental data has been measured with respect to the TEM balance pivot point and therefore

$$\left(\frac{dC_{M_p}}{dC_L} \right)_{\text{stick fixed}} = (h_p - h_n) \quad \text{EQN. (17)}$$

A graph of $\frac{dC_{M_p}}{dC_L}$ for the tail-on configuration was plotted for each tailplane setting angle η . The linear region of this graph is shown over leaf in Fig. 13. The gradient of the lines was found to be:

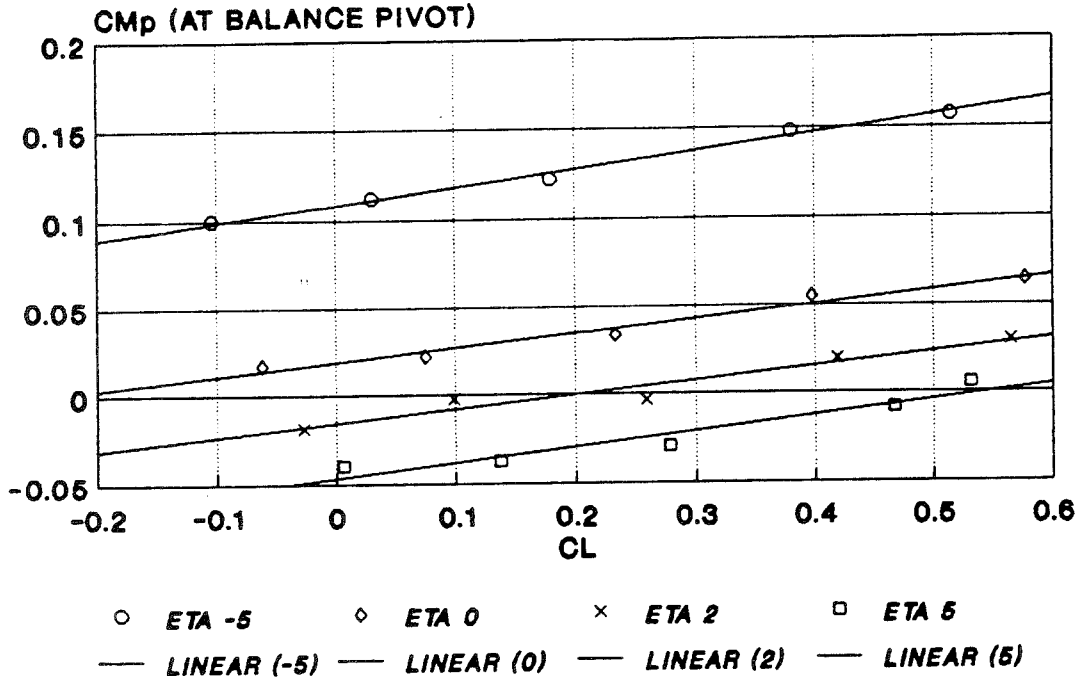
$$\left(\frac{dC_{M_p}}{dC_L} \right)_{\text{stick fixed}} = (h_p - h_n) = 0.081$$

As $h_p = 0.797\bar{c}$, the position of the neutral point was then estimated to be:

$$\underline{h_n = 0.716\bar{c} \quad \text{ie. 106mm aft of the reference line.}}$$

FIG. 13: C_M vs C_L (TAIL-ON FOR VARIOUS η).

AVERAGE $dC_M/dC_L : + 0.081 : h_p - h_n$



3.5 FURTHER CONFIRMATION OF THE VALUE OF h_n .

From the previous sections, the values of all the following parameters are known:

$$\begin{aligned} \bar{V} &= 0.61 & d\epsilon/d\alpha_t &= 0.57 \\ a_1 &= dC_{L_t}/d\alpha_t = 0.04 & a &= dC_L/d\alpha = 0.065 \\ h_o &= 0.543\bar{C} & & \text{ie. 80.4 mm aft of the reference line.} \end{aligned}$$

Therefore, it is possible to find h_n by substituting these values into Eqn. 15 below:

$$\bar{V} \frac{a_1}{a} \left(1 - \frac{d\epsilon}{d\alpha} \right) = (h_n - h_o)$$

to get: $h_n = 0.704\bar{C}$ ie. 104.3 mm aft of the reference line.

3.6 DISCUSSION.

Using the slope of dC_{M_p}/dC_L and equation 15 to estimate the value of h_n gave two different values of $h_n = 0.716\bar{c}$ and $0.704\bar{c}$ respectively. This is just a difference in location of 1.7mm. Given the experimental errors involved in measuring h_p , C_{M_p} , C_L and all the various slopes of graphs etc., the difference is surprisingly small.

The position of the model gimbal and c.g. was difficult to measure and was estimated to be 101.5 mm aft of the reference line (ie. $h = 0.686\bar{c}$). Therefore, whatever value of h_n is taken, it can still be seen that the difference in position between the gimbal pivot point and the neutral point of the model is of the order of a few mm. This confirmed the observation that the model was very difficult to trim as it is very close to being neutrally stable. All of the C_{M_p} vs C_L curves shown up to now have had positive slopes indicating that the model is unstable. However, this is due to the pitching moment C_{M_p} being measured at the balance pivot which is 12-14 mm aft of the neutral point of the model.

To confirm that the model is approximately neutrally stable values of the pitching moments and coefficients were calculated at the gimbal/c.g. point on the model (ie. 16.5 mm in front of the TEM balance pivot point.) This was done by modifying the BASIC program used to produce the original values of C_L , C_d and C_{M_p} from experimental data. Pitching moment coefficients (C_{M10} and C_{M15}) were also calculated at 10mm and 15mm in front of the current gimbal/c.g. position.

Graphs of C_M vs C_L were then plotted for various points aft of the reference line of the model and these are presented in Appendix A. The graphs show quite clearly how the static stability changes with reference point. A graph of C_M vs C_L at various positions, for tailplane angle $\eta_t = 0^\circ$, has been constructed and is shown over leaf in FIG. 14. It may be seen that at the model neutral point the graph is almost horizontal with a slope of -0.001.

At the model gimbal/c.g. the slope is slightly negative with $dC_M/dC_L = -0.03$. This means that the distance to the neutral point from the centre of the gimbal is only 4.4 mm. The gimbal position is more important than the c.g. position. At 10 mm and 15 mm in front of the current gimbal position the stability of the model is increased, as may be seen by the more negative slopes of FIG.14.

The distance that the gimbal can be moved is restricted by the construction of the model. It was therefore decided, on the basis of the above analysis, to move the gimbal forward 10 mm. This has also involved a small enlargement of the open central access hole of the model to enable adequate clearance of the vertical support rod which passes through the centre of the model and gimbal.

Finally, FIG. 15 over leaf summarises the various distances and positions which have been found through this longitudinal static stability analysis.

FIG. 14: C_M vs C_L ($\eta = 0$, VARIOUS POSITIONS).

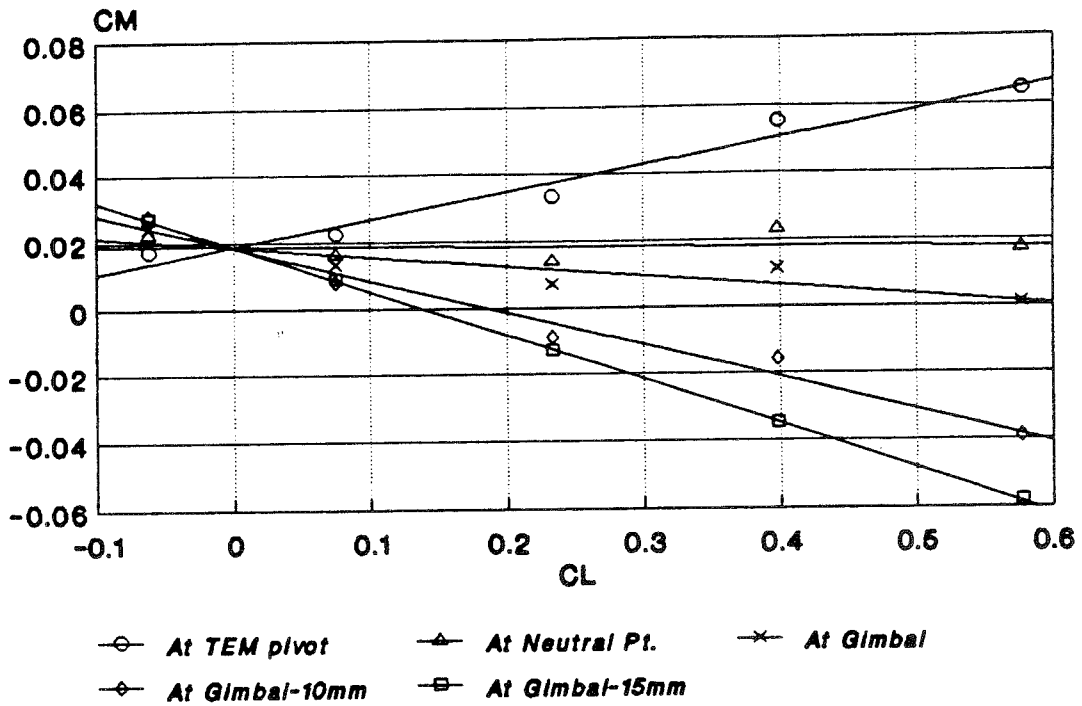
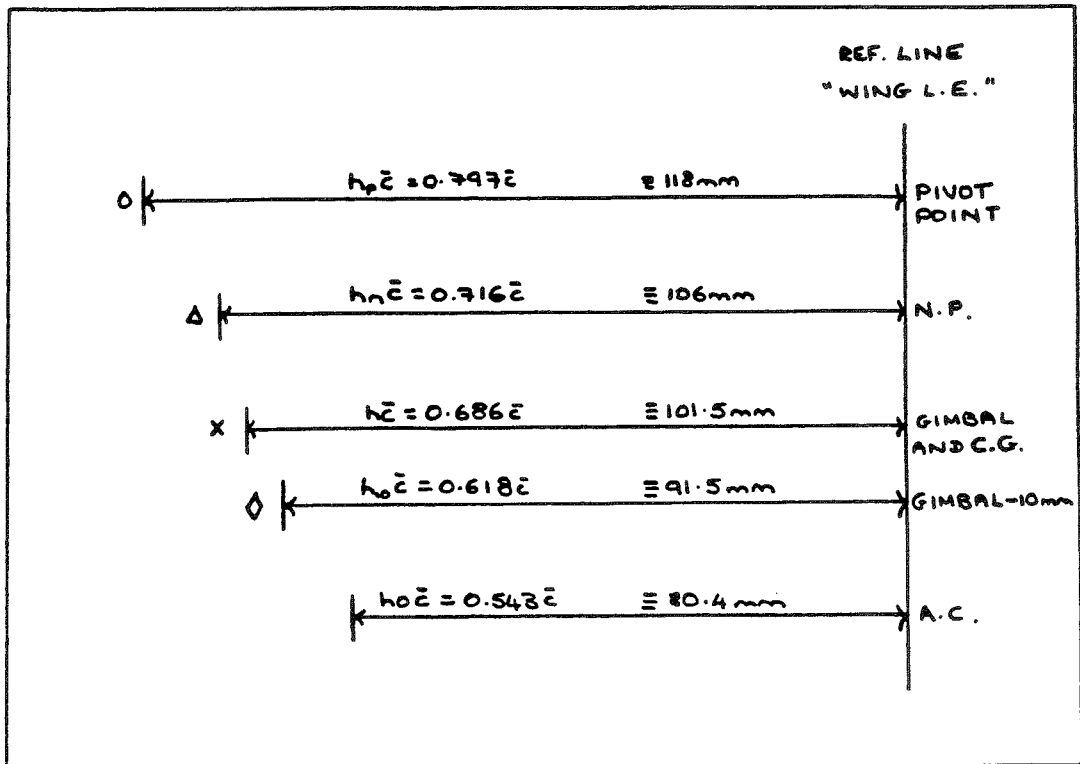


FIG. 15: SUMMARY OF IMPORTANT POINTS ON THE HAWK MODEL.



4.0 AIRCRAFT/MODEL SCALING LAWS.

Whenever a scaled model is used to investigate the dynamic behaviour of a full scale aircraft it is necessary to be able to correlate results between the two aircraft in some way. To ensure a realistic representation of the full scale aircraft the similarity parameters required are usually found in a non-dimensional form by considering the relevant equations of motion or by the use of dimensional analysis.

For geometric similarity, the model must have the same shape as the full scale aircraft with the ratio of all linear dimensions (l_m/l_a) being constant. Kinematic similarity involves the consideration of aerodynamic characteristics and the scaling of linear and angular acceleration and velocity. Dynamic similarity exists when the geometric and kinematic similarities are satisfied and the ratio of all the forces are the same.

For example, the aerodynamic forces can be represented in the following form:

$$\text{Force} = f_1(\rho, L, \nu, V)$$

in which f_1 is a function of density, ρ , a length, L , kinematic viscosity ν and velocity V , (reference 3). However, when comparing aircraft manoeuvring, gravity (g), must be taken into account. Also, if an aircraft is moving fast enough then Mach number is included so that:

$$\text{Force} = \rho \cdot L^2 \cdot V^2 \cdot f_2 \left(\frac{VL}{\nu}, \frac{V}{a}, \frac{V^2}{Lg} \right)$$

where the terms in the brackets will be recognised as:

(i) Reynolds Number, $Re = \rho L V / \mu$

(ii) Mach Number, $M = V/a$

(iii) Froude Number, $F = V^2/gL$

Complete dynamic simulation can only be achieved when the following dimensionless parameters are numerically equal for both the model and the full size aircraft, references 4 and 5 :

1. Scale Factor:

The geometric scale factor, λ , is the constant ratio which relates all aircraft lengths (l_m) and model lengths (l_a) as shown below. For the B.Ae. Hawk model $\lambda = 1/12$.

$$\lambda = \frac{l_m}{l_a}$$

2. Mach Number:

The Mach Number, M , is expressed as the ratio of fluid velocity to its local speed of sound (a) :

$$M = \frac{V}{a}$$

This number takes into account the compressibility effect of the airflow. The Weybridge tunnel which will be used with the Hawk model is only a low speed tunnel and as $M < 0.4$ with this facility the compressibility effects may be neglected.

3. Relative Density Factor and Mass Scaling:

The relative density factor μ_L allows for correct mass scaling for a given set of flight conditions and is defined as:

$$\mu_L = \frac{2m}{\rho S l_\mu}$$

where: m = mass; ρ = air density; S = wing area;
 l_μ = fuselage length.

The ratio of model to aircraft mass may be expressed as:

$$m_m = m_a \cdot (\lambda)^3$$

4. Relative Radius of Inertia Factor:

For correct dynamic response the relative radius of inertia, K_y must be the same for both the model and aircraft. K_y is defined by

$$K_y = \left(\frac{r_y}{T \mu} \right) \quad \text{where } r_y = \text{radius of inertia.}$$

Further, if λ is correct $r_{y_m} = r_{y_a} \cdot (\lambda)$

5. Froude Number:

The Froude Number, F_r , scales the effect of gravity on the aircraft model and is defined as the ratio of inertia to gravity forces as follows:

$$F_r = \frac{V}{\sqrt{1 \mu g}}$$

where V is the velocity of the c.g. and g = acceln. due to gravity

When the Froude Number is combined with the relative density parameter μ_L , the lift coefficient for steady flight C_{L_0} can be found:

$$C_{L_0} = \frac{\mu_L}{F_r^2} = \frac{2mg}{\rho S V^2}$$

To ensure that the model model aircraft flies at the same reference angle of attack as the full scale aircraft $F_{r_m} = F_{r_a}$ and correct mass scaling is required. Further, Froude number equality results in the following expression for the ratio of aircraft and model velocity:

$$\frac{V_m}{V_a} = \sqrt{\lambda} \cdot \sqrt{g_m/g_a}$$

where g_m = model gravity and g_a = aircraft gravity.

Thus the model velocity is dependent on the scale factor (λ) and the ratio of gravitational forces. Supporting part of the model weight allows a reduction in tunnel speed to simulate similar aircraft velocities. The use of an artificial 'g' control system for the Hawk dynamic wind tunnel facility has been the subject of a recent MSc thesis at Cranfield, reference 5.

6. Reynolds Number:

The Reynolds Number, Re , is the ratio of inertia to viscous forces and is defined as:

$$Re = \frac{\rho \cdot l \cdot V}{\mu} \quad \text{where } \mu = \text{viscosity of air.}$$

Using the relationship $\nu = \mu/\rho$ where ν = the coefficient of kinematic viscosity of air, enables Re to be expressed as:

$$Re = \frac{l \cdot V}{\nu}$$

Hence
$$\frac{Re_m}{Re_a} = \frac{l_m \cdot V_m}{l_a \cdot V_a} \quad \text{and if } g_m \text{ is assumed equal to } g_a$$

then
$$\frac{Re_m}{Re_a} = (\lambda)^{3/2} \quad \text{for the same altitude conditions.}$$

From this last equation it is clear that Re can never be the same for the full scale aircraft and the scaled model because of the scale factor $\lambda^{3/2}$. To achieve both dynamic similarity and a reasonable test Reynolds number requires the use of very large models. Therefore it is common practice to just ensure that Re in the wind tunnel is higher than $Re = 0.4 \times 10^6$, which is the critical value at which the flow becomes turbulent.

4.1 SUMMARY OF SIMILARITY LAWS.Optional Parameters

1. Model Scale
2. Speed
3. Density

Scale

$$l_m/l_a = \lambda$$

$$V_m/V_a = (\lambda)^{1/2}$$

$$\rho_m/\rho_a (=1 \text{ for Hawk model})$$

Required Scaling

4. Mass
5. Inertia
6. Gravity

Relationship

$$\frac{M_m}{M_a} = \frac{\rho_m}{\rho_a} (\lambda^3)$$

$$\frac{I_m}{I_a} = \frac{\rho_m}{\rho_a} (\lambda^5)$$

$$\frac{g_m}{g_a} = \frac{1}{\lambda} \left(\frac{V_m}{V_a} \right)^2$$

Analysis of Resultant Motion

7. Time
8. Linear Displacement
9. Angular Displacement
10. Linear Velocity
11. Angular Velocity
12. Linear Acceleration
13. Angular Acceleration

Relationship

$$\frac{t_m}{t_a} = \tau = \frac{V_a}{V_m} \lambda = (\lambda)^{1/2}$$

$$\frac{x_m}{x_a} = \lambda$$

$$\frac{\theta_m}{\theta_a} = 1$$

$$\frac{\dot{x}_m}{\dot{x}_a} = \frac{\lambda}{\tau} = (\lambda)^{1/2}$$

$$\frac{\dot{\theta}_m}{\dot{\theta}_a} = \frac{1}{\tau}$$

$$\frac{\ddot{x}_m}{\ddot{x}_a} = \frac{\lambda}{\tau^2}$$

$$\frac{\ddot{\theta}_m}{\ddot{\theta}_a} = \frac{1}{\lambda^2}$$

4.2 SCALING OF DERIVATIVES.

In order to directly compare the magnitudes of the stability and control derivatives, the derivatives are first expressed in a non-dimensional form and then further reduced to the concise form defined overleaf, reference 6. The non-dimensional form of the equations of motion use these concise derivatives as well as a non-dimensional time, \hat{t} and non-dimensional inertia parameters.

4.2.1 NON-DIMENSIONAL MASS AND INERTIA.

Non-dimensional time \hat{t} is given by: $\hat{t} = t/\tau$

where $\tau = m/0.5\rho VS = V_e C_L / g \cdot \cos(\theta_e)$

The aircraft longitudinal relative density parameter is given by:

$$\mu_1 = m/0.5\rho S \bar{c} = V\tau/\bar{c}$$

where \bar{c} is the mean aerodynamic chord of the wing.

The aircraft lateral relative density parameter is given by:

$$\mu_2 = m/0.5\rho S b = V\tau/b$$

where b is the wing span.

The non-dimensional inertia parameters are as follows:

non-dimensional rolling moment of inertia, $i_x = I_x/mb^2$

non-dimensional pitching moment of inertia, $i_y = I_y/m\bar{c}$

non-dimensional yawing moment of inertia, $i_z = I_z/mb^2$

non-dimensional product of inertia about O_x & O_z , $i_{zx} = I_{zx}/mb^2$

4.2.2 CONCISE LONGITUDINAL DERIVATIVES.

<u>concise</u>		<u>non-dimensional</u>
$x_u = X_u \cdot (-1)$	where	$X_u = \hat{X}_u / 0.5\rho V S$
$x_w = X_w \cdot (-1)$	where	$X_w = \hat{X}_w / 0.5\rho V S$
$x_w^\bullet = X_w^\bullet \cdot (-1/\mu_1)$	where	$X_w^\bullet = \hat{X}_w^\bullet / 0.5\rho S \bar{C}$
$x_q = X_q \cdot (-1/\mu_1)$	where	$X_q = \hat{X}_q / 0.5\rho V S \bar{C}$
$x_\eta = X_\eta \cdot (-1)$	where	$X_\eta = \hat{X}_\eta / 0.5\rho V^2 S$
$z_u = Z_u \cdot (-1)$	where	$Z_u = \hat{Z}_u / 0.5\rho V S$
$z_w = Z_w \cdot (-1)$	where	$Z_w = \hat{Z}_w / 0.5\rho V S$
$z_w^\bullet = Z_w^\bullet \cdot (-1/\mu_1)$	where	$Z_w^\bullet = \hat{Z}_w^\bullet / 0.5\rho S \bar{C}$
$z_q = Z_q \cdot (-1/\mu_1)$	where	$Z_q = \hat{Z}_q / 0.5\rho S \bar{C}$
$z_\eta = Z_\eta \cdot (-1)$	where	$Z_\eta = \hat{Z}_\eta / 0.5\rho V^2 S$
$m_u = M_u \cdot (-\mu_1/i_y)$	where	$M_u = \hat{M}_u / 0.5\rho V S \bar{C}$
$m_w = M_w \cdot (-\mu_1/i_y)$	where	$M_w = \hat{M}_w / 0.5\rho V S \bar{C}$
$m_w^\bullet = M_w^\bullet \cdot (-1/i_y)$	where	$M_w^\bullet = \hat{M}_w^\bullet / 0.5\rho S \bar{C}^2$
$m_q = M_q \cdot (-1/i_y)$	where	$M_q = \hat{M}_q / 0.5\rho V S \bar{C}^2$
$m_\eta = M_\eta \cdot (-\mu_1/i_y)$	where	$M_\eta = \hat{M}_\eta / 0.5\rho V^2 S \bar{C}$

4.2.3 CONCISE LATERAL DERIVATIVES.concise

$$y_v = Y_v \cdot (-1)$$

$$y_p = Y_p \cdot (-1/\mu z)$$

$$y_r = Y_r \cdot (-1/\mu z)$$

$$y_\xi = Y_\xi \cdot (-1)$$

$$y_\zeta = Y_\zeta \cdot (-1)$$

$$l_v = L_v \cdot (-\mu z/i_x)$$

$$l_p = L_p \cdot (-1/i_x)$$

$$l_r = L_r \cdot (-1/i_x)$$

$$l_\xi = L_\xi \cdot (-\mu z/i_x)$$

$$l_\zeta = L_\zeta \cdot (-\mu z/i_x)$$

$$n_v = N_v \cdot (-\mu z/i_z)$$

$$n_p = N_p \cdot (-1/i_z)$$

$$n_r = N_r \cdot (-1/i_z)$$

$$n_\xi = N_\xi \cdot (-\mu z/i_z)$$

$$n_\zeta = N_\zeta \cdot (-\mu z/i_z)$$

where

where

where

where

where

where

where

where

where

where

where

where

where

where

where

non-dimensional

$$Y_v = \hat{Y}_v / 0.5\rho V S$$

$$Y_p = \hat{Y}_p / 0.5\rho V S b$$

$$Y_r = \hat{Y}_r / 0.5\rho V S b$$

$$Y_\xi = \hat{Y}_\xi / 0.5\rho V^2 S$$

$$Y_\zeta = \hat{Y}_\zeta / 0.5\rho V^2 S$$

$$L_v = \hat{L}_v / 0.5\rho V S b$$

$$L_p = \hat{L}_p / 0.5\rho V S b^2$$

$$L_r = \hat{L}_r / 0.5\rho V S b^2$$

$$L_\xi = \hat{L}_\xi / 0.5\rho V^2 S b$$

$$L_\zeta = \hat{L}_\zeta / 0.5\rho V^2 S b$$

$$N_v = \hat{N}_v / 0.5\rho V S b$$

$$N_p = \hat{N}_p / 0.5\rho V S b^2$$

$$N_r = \hat{N}_r / 0.5\rho V S b^2$$

$$N_\xi = \hat{N}_\xi / 0.5\rho V^2 S b$$

$$N_\zeta = \hat{N}_\zeta / 0.5\rho V^2 S b$$

5.0 MEASUREMENT OF MOMENTS OF INERTIA.

It was decided to measure the Hawk models' moments of inertia using a free oscillation method, as used in references 7 and 8. In this method the Hawk is mounted horizontally on its' vertical rod within the dexion framework of the dynamic rig. The model and rod are free to rotate about the centre line of the rod. The model is suitably restrained by springs attached to the dexion framework from the aft of the aircraft model or from a wing, depending on which moment of inertia is being sought.

The model and framework is placed in the wind tunnel and the model is deflected from the zero equilibrium condition. Upon release, the model will perform a damped oscillatory motion whose amplitude and frequency is dependent on the relevant stability derivatives, (eg. N_v & N_r), the restraining spring characteristics and the friction in the mounting. The oscillations may be recorded using a graph plotter and suitably analysed for wind-on and wind-off conditions in the wind tunnel. Oscillations with wind on will yield the appropriate stability derivatives. When the wind is off, the stability derivatives are assumed to be approximately zero and the moment of inertia and mechanical friction terms may be found.

The following theory is presented for the case where the model is oscillating laterally in yaw. The equations for the pitch and roll oscillations are very similar.

Choosing the directional reference axis to coincide with the wind direction in the tunnel, then

$$\psi = -\beta \quad \text{EQN. (18)}$$

and the side slip velocity is

$$v = -U_\infty \psi$$

$$v = -U_\infty \tan\beta \approx -U_\infty \beta \quad \text{EQN. (19)}$$

where, in the experiment, U_∞ is the *tunnel speed*.

During the oscillation these three terms contribute yawing moment to the motion: these are :-

- $I_z \cdot (d^2\psi/dt^2)$ *inertial moment.*
 $-(N_r - f_z) \cdot d\psi/dt$ *sum of damping in yaw and rig friction.*
 $(U\omega \cdot N_v + K) \cdot \psi$ *sum of aerodynamic and restraining spring moment.*

where:

- I_z *moment of inertia and model about z-axis.*
 f_z *mechanical friction moment / unit angular velocity.*
 K *restraining spring stiffness where: $K = l^2(k_1 + k_2)$*
 l *distance along the model axis from the pivot point to the point on the model that is connected to the restraining springs.*
 k_1 *restraining spring constant (port side).*
 k_2 *restraining spring constant (starboard side).*
 N_r *yawing moment due to rate of yaw $\delta N / \delta r$.*
 N_v *yawing moment due to rate of side slip $\delta N / \delta v$.*

Equating the contributions above gives the yawing eqn. of motion:

$$\boxed{I_z \cdot \frac{d^2\psi}{dt^2} - (N_r - f_z) \frac{d\psi}{dt} + (U\omega N_v + K) \cdot \psi = 0} \quad \text{EQN. (20)}$$

Equation (20) may be expressed in the form:

$$\frac{d^2\psi}{dt^2} + a \cdot \frac{d\psi}{dt} + b \cdot \psi = 0 \quad \text{EQN. (21)}$$

where:

$$\boxed{a = -(N_r - f_z) / I_z}$$

and

$$\boxed{b = (U\omega N_v + K) / I_z}$$

Equation (20) may also be expressed in the form:

$$\frac{d^2\psi}{dt^2} + 2\zeta\omega_o \cdot \frac{d\psi}{dt} + \omega_o^2 \cdot \psi = 0 \quad \text{EQN. (22)}$$

where: ζ = system damping ratio.
 ω_o = system undamped natural frequency.

Comparing (21) and (22) gives:

$$a = 2\zeta\omega_o = -(N_r - f_z)/I_z \quad \text{EQN. (23)}$$

$$\text{and } b = \omega_o^2 = (U\omega N_v + K)/I_z \quad \text{EQN. (24)}$$

If the model is tested with the wind-off, the aerodynamic terms of equation (20) may be neglected since $N_v \approx 0$ and $N_r \approx 0$. Further, $U\omega$ will be zero and the following terms may be defined for the wind-off case:

$$\mu = -\zeta\omega_o = f_z/2 \cdot I_z \quad \text{EQN. (25)}$$

$$\omega_o^2 = [I^2(k_1 + k_2)]/I_z \quad \text{EQN. (26)}$$

A general solution to the oscillatory motion of Eqn.(22) may be expressed in the following way:

$$\psi = A_o \cdot e^{-\mu t} \cdot \cos(\omega_d t + \delta) \quad \text{EQN. (27)}$$

where:

δ is some initial yaw angle on the recorded oscillations and the system damped natural frequency is given by

$$\omega_n = \omega_o \cdot (1 - \zeta^2)^{1/2} = \frac{2\pi}{T} \quad \text{EQN. (28)}$$

T = period of oscillatory motion (wind-off).

From Eqn.(25) $\zeta^2 = (\mu)^2/(\omega_0)^2$

and substituting this into Eqn.(28) gives:

$$\omega_0^2 \cdot \left[1 - \frac{\mu^2}{\omega_0^2} \right] = \frac{4\pi^2}{T^2}$$

$$\Rightarrow \omega_0 = \left[\omega_n^2 + \mu^2 \right]^{1/2} = \left[\frac{4\pi^2}{T^2} + \mu^2 \right]^{1/2} \quad \text{EQN. (29)}$$

GRAPHICAL ANALYSIS OF THE RECORDED OSCILLATIONS.

The damped oscillations of the model which are recorded by the graph plotter will be of the form:

$$\psi = A_0 \cdot e^{-\mu t} \cdot \cos(\omega_n t + \delta)$$

When the term $\cos(\omega_n t + \delta) = 1$, this will correspond to the maximum and minimum peaks of the recorded oscillations. Thus taking any two maximum peaks, A_1 and A_2 at times t_1 and t_2 , it is possible to calculate μ from the following formula:

$$\ln \left(\frac{A_1}{A_2} \right) = \mu \cdot (t_2 - t_1) \quad \text{EQN. (30)}$$

Again from the recorded oscillations, knowing the graph plotter pen sweep rate, enables the damped period T of the motion to be found. Substituting the values of T and μ into Eqn.(29) will yield the natural frequency of oscillation ω_0 . Then, from Eqn.(26) and Eqn.(25) respectively, I_z and f_z may be found:

$$I_z = [l^2(k_1 + k_2)]/(\omega_0^2) \quad \text{EQN. (31)}$$

$$\mu = f_z = 2 \cdot I_z \cdot \mu \quad \text{EQN. (32)}$$

5.1 PITCH INERTIA.

All of the inertia experiments described below were carried out for the wind-off condition only. To measure the pitch inertia two springs were attached vertically between the aft of the model and the dexion framework using very stiff wire, similar to piano wire. The distance from the centre of the vertical rod through the model gimbal to the aft attachment point was $l = 0.4\text{m}$. Various springs were attached to the model to see which gave the best vertical oscillations in pitch when the model was disturbed from its zero rest position. The two springs which were finally used had spring constants of $k_1 = 8.9 \text{ N/m}$ and $k_2 = 6.2 \text{ N/m}$. The spring constants were measured by recording the spring length for various masses which were hung from the spring. Then assuming a simple law of force = $k \times$ extension, k was calculated from the slope of the appropriate graphs as shown in Figures B-1 and B-2 of Appendix B.

The Hawk model was set in oscillation and the decay curve recorded by a graph plotter by recording the variation in pitching angle θ from the dynamic rig electronic control unit. The output was therefore in volts. But as only the period and damping is required the amplitude of the motion may be in any arbitrary unit. The average period of the oscillation was measured from the response graph and converted to seconds using:

$$T = d/sr = 25/20 = \underline{1.25 \text{ sec}} \quad \text{EQN. (33)}$$

where: d = period in mm and sr = pen sweep rate in mm/sec

Next, the values of the maximum peaks were estimated from the decay graph and plotted against time. An exponential curve of the form $x = A_0 e^{-\mu t}$ was fitted to these points, shown in figure B-3 and the value of μ found using Eqn.30:

$$\mu = \ln \left(\frac{35.352}{29.231} \right) + (9.735 - 5.625) = \underline{0.046 \text{ (rad/sec)}}$$

There are two other ways in which μ may be found. By finding the time from peak to half amplitude μ will equal $\Delta t/0.693$. Alternatively, a graph of $\ln(A_n/A_{n+1})$ vs. t will yield a straight line of gradient μ . Both of these methods yielded $\mu \approx .046 \text{ rad.s}^{-1}$.

The values of T and μ were then substituted in Eqn.29:

$$\omega_o^2 = (\omega_n^2 + \mu^2) = \frac{4\pi^2}{T^2} + \mu^2 = (5.0265)^2 + (0.046)^2 = \underline{25.268 \text{ (rad/sec)}^2}$$

It was noted that the natural frequency of oscillation is not very much different to the damped frequency as μ is so small.

Finally, using Equations 31 and 32, the values of I_y and f_y were found:

$$(i) \quad I_y = [l^2(k_1 + k_2)]/(\omega_o^2) \quad \rightarrow \quad \underline{I_y = 0.0956 \text{ kgm}^2 \text{ or } 0.07 \text{ slug.ft}^2}$$

$$(ii) \quad f_y = 2.I_y.\mu \quad \rightarrow \quad \underline{f_y = 0.0088 \text{ kgm}^2.\text{rad/sec}}$$

Nb. f_y is the mechanical friction moment / unit angular vel.

From reference 9, I_{y_a} was estimated to be 19534.4 kgm^2 . The scale law for inertia is $I_m = \lambda^5.I_a$ and this implies that the model moment of inertia should be $I_{ym} = 0.079 \text{ kgm}^2$ or $.058 \text{ slug.ft}^2$. The fact that the theoretical and measured inertias do not agree is probably because the pitch inertia is most sensitive to longitudinal variations in mass and there are a number of weights which had been added to the model to locate the c.g. at the gimbal centre and allow the model to be mounted on the TEM force balance. Now that the longitudinal static stability experiments have finished the extra model 'weights' will be removed and all of the moments of inertia experiments will be repeated. Also, with the model gimbal repositioned 10mm in front of its previous position, the model should be more stable and the experiments may also be performed with the wind-on to give estimates of derivatives such as N_v and N_r .

5.2 ROLL INERTIA.

To measure the roll inertia the two springs were attached vertically to the port wing of the model, with one spring above and the other spring below the wing. The spanwise distance along the wing from the vertical rod and gimbal was measured to be $l = 0.22\text{m}$. The model was set in oscillation and the decay recorded using the electronic control unit and graph plotter. From this decay graph the period of oscillation was found using:

$$T = d/sr = 52.5/50 = \underline{1.05 \text{ sec}}$$

Next, the values of the maximum peaks were estimated from the decay graph and plotted against time. An exponential curve was fitted to the points, as shown in figure B-4. The values of μ and ω_0^2 were calculated in the same way as before.

$$\mu = \ln\left(\frac{55.292}{18.684}\right) + (5.425 - 1.225) = \underline{0.258 \text{ (rad/sec)}}$$

$$\omega_0^2 = (\omega_n^2 + \mu^2) = \frac{4\pi^2}{T^2} + \mu^2 = (5.984)^2 + (0.258)^2 = \underline{35.875 \text{ (rad/sec)}^2}$$

Finally, using Equations 31 and 32, the values of I_x and f_x were found as follows:

$$(i) \quad I_x = [l^2(k_1 + k_2)]/(\omega_0^2) \rightarrow \underline{I_x = 0.0204 \text{ kgm}^2 \text{ or } 0.015 \text{ slug.ft}^2}$$

$$(ii) \quad f_x = 2.I_x.\mu \rightarrow \underline{f_x = 0.0105 \text{ kgm}^2.\text{rad/sec}}$$

From reference 9, for the scale Hawk aircraft I_{x_a} is equal to 5346.7 kgm^2 , which implies that for the model $\underline{I_{x_m} = 0.016 \text{ slugft}^2}$. Therefore, there is a good agreement between the theoretical and measured rolling moment of inertia.

5.3 YAW INERTIA.

To measure the yawing moment of inertia two springs were attached horizontally to the aft of the model at $l = 0.4\text{m}$ from the vertical rod. The model was set in lateral oscillation and the decay curve recorded. However, it was not possible to obtain a proper decay curve from the model for two main reasons. The yawing motion is subject to a fairly large mechanical friction because of the way that the vertical rod supporting the model must be restrained at the top of the dexion framework. Therefore, the motion tends to damp out very quickly.

The second problem is due to the way in which the yaw attitude potentiometer is fitted to the rig. The small moving bar or the potentiometer is slotted into the bottom of the vertical support rod with the main body of the potentiometer being fixed to a stationary horizontal disc on the rig using insulating tape. The potentiometer was difficult to secure in position and did not remain at all stationary. Therefore, it will be necessary to fill the gap around of the potentiometer with foam to ensure that the main body will not move.

Both of these problems will be rectified before the next set of experimental tests using the model.

6.0 DATA ACQUISITION SYSTEM.

When data from the electronic control unit is recorded on disk on the IBM computer using the CED 1401 analogue-to-digital conversion system, the data is in the form of 16 bit signed words. This data must be converted into voltages and information from the various channels of the CED 1401 in use must be combined into a single file suitable for use by the MSR method. Furthermore, the data in the file must be changed to represent physical parameters, such as pitch attitude angle, by multiplying the voltages by the appropriate calibration constants. A BASIC program has been written to accomplish this and a listing of this program is given in Appendix C. However, until the calibrations of the control surface and attitude angles are complete, the program leaves the output data in the form of voltages.

The dynamic rig was initially designed so that the attitude angles of the Hawk model may be accurately measured using various potentiometers. Size constraints on the scaled model meant that it was not feasible to insert rate gyros into the model. Thus any attitude angle rate data required has to be generated using either analogue or digital methods. Reference 2 suggests a number of ways to generate the rate data required. One numerical method, based on a Taylor Series expansion will differentiate data using the following formula:

$$y'_i = \frac{-y_{i+2} + 8y_{i+1} - 8y_{i-1} + y_{i-2}}{12h} \quad \text{EQN. (34)}$$

This equation requires five consecutive data points in order to calculate the approximate derivative (y'_i) at the central point x_i . This means that the first two points of any recorded data will always be lost. The error of the above expression is of order h^4 and should be small if the time (h) between data points is small.

It was decided to incorporate Eqn.34 into the BASIC program of Appendix C. Therefore, when the program asks which channels from the CED are to be combined into a single file, it also asks if any channels require differentiation. The program has been tested with 'made up data' so far and it is hoped to test it with real data in the near future.

7.0 CONCLUSION.

As a result of the longitudinal stability analysis for the Hawk model the position of the gimbal has been moved forward 10mm. This should make the model more stable and easier to control in the tunnel. It is planned to test the model in the tunnel in the near future and also to repeat the moment of inertia experiments.

Calibrations of the input and output voltages for the control surfaces and attitude angles will be performed in order to complete the BASIC program for conversion of data into the format required by the MSR program.

During the next quarter it is planned to fly the model in the wind tunnel and to record the model's response to various control surface inputs. This data will then be analysed using the MSR FORTRAN 77 program to obtain as many stability and control derivatives as possible. Various methods to produce attitude angle rate data will be implemented.

REFERENCES.

1. KLEIN, V.; BATTERSON, J.G.; and MURPHY, P.C.: Determination of Airplane Model Structure from Flight Data by Using Modified Stepwise Regression. October 1981. NASA TP1916.
2. HINDS, H.A. and COOK, M.V.: Preliminary Studies for Aircraft Parameter Estimation using Modified Stepwise Regression. College of Aeronautics Report No P8911, Cranfield Institute of Technology, November 1989.
3. STINTON, D.: The Design of the Aircraft, BSP Professional Books, 1983.
4. MALIK, I.A.: The Design, Development and Evaluation of an Active Control Aircraft Model Wind Tunnel Facility. 1982 College of Aeronautics Ph.D. Thesis, Cranfield Institute of Technology.
5. FILMER, S.W.: An Artificial "g" Control System for the Dynamic Wind Tunnel Facility. College of Aeronautics MSc Thesis, Cranfield Institute of Technology, 1989.
6. BABISTER, A.W.: Aircraft Dynamic Stability and Response. Pergamon Press, 1980.
7. COLLEGE OF AERONAUTICS: The Determination of N_v and N_r by the Free Oscillation Method. Unpublished College of Aeronautics Laboratory Handout.
8. GOMES, S.B.V.: Task 3: Measurement of Some Aerodynamic Damping Derivatives for the YEZ-2A Airship. Unpublished College of Aeronautics Report No. NFP8909, Cranfield Institute of Technology, May 1989.
9. HINDS, H.A. and COOK, M.V.: Third Quaterly Report on the Application of Modified Stepwise Regression for the Estimation of Aircraft Stability and Control Parameters. College of Aeronautics Report No. 9008, Cranfield Institute of Technology, April 1989.

APPENDIX A:

C_M v C_L STABILITY LINES AT DIFFERENT POSITIONS.

$d_{CM}/d_{CL} : -0.001$

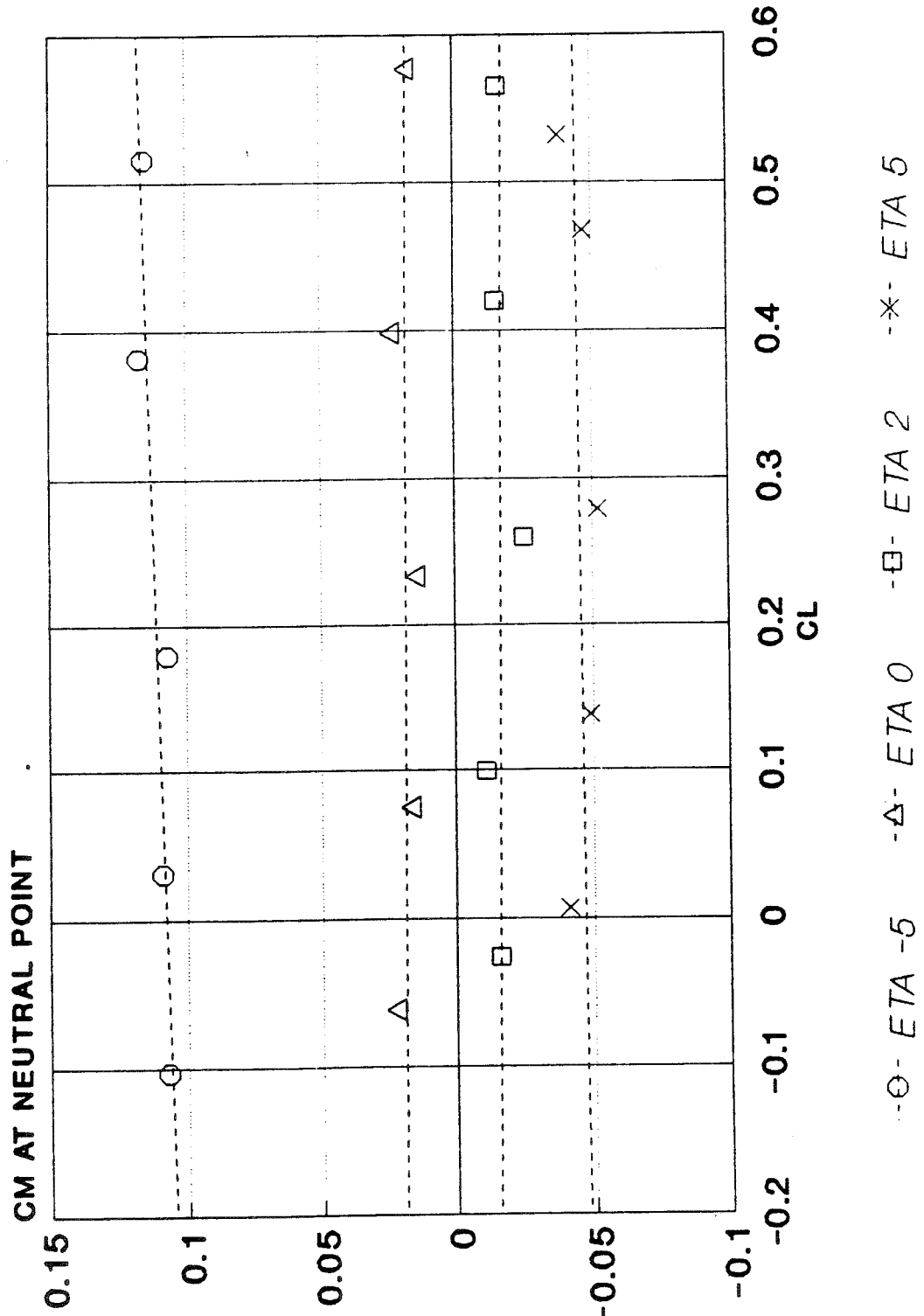


FIG. A-1: CM vs CL (AT NEUTRAL POINT)

$dCM/dCL : -0.03$

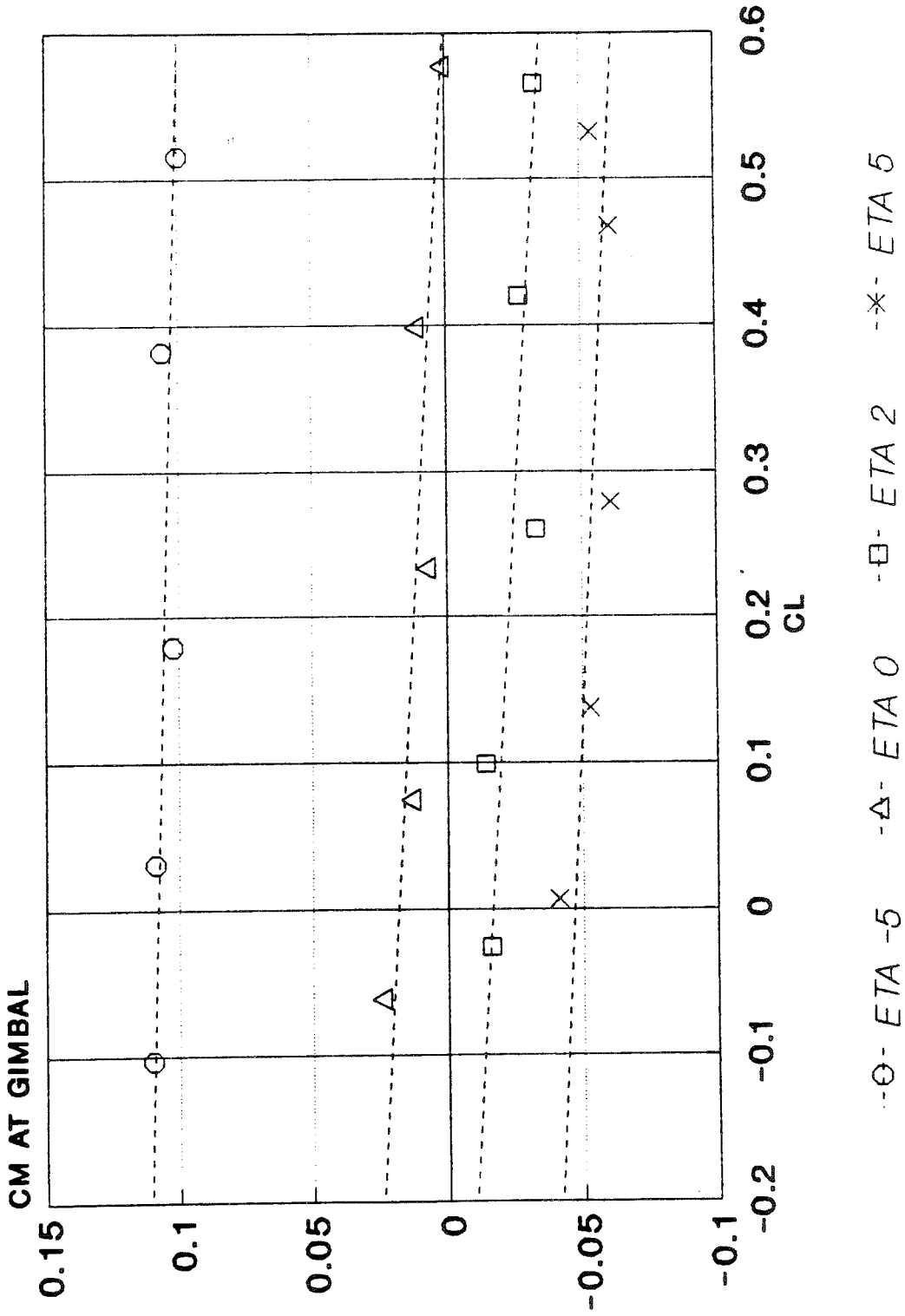


FIG. A-2: CM vs CL (AT GIMBAL / C.G.)

$dCM/dCL : -0.099$

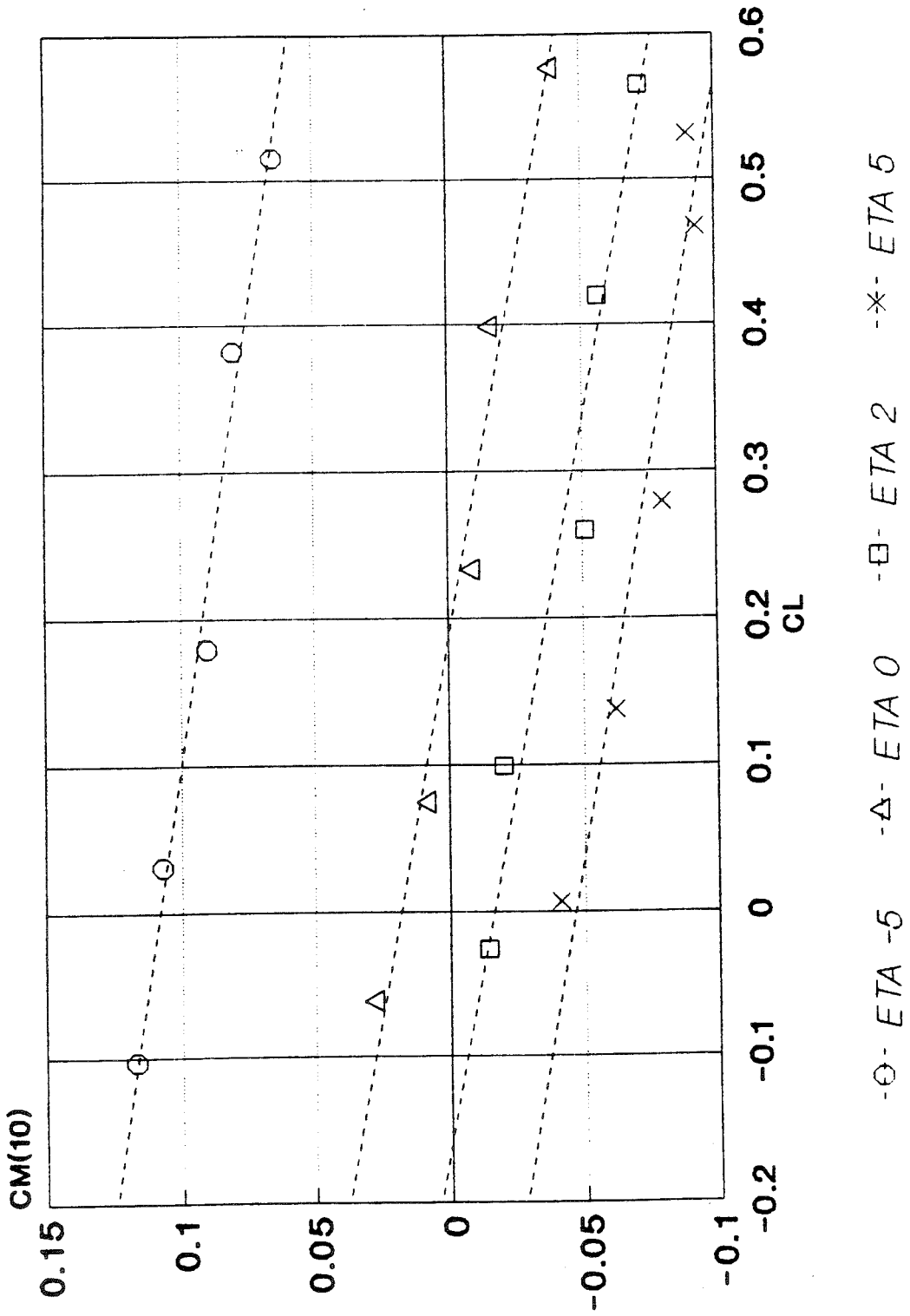


FIG. A-3: CM vs CL (10mm BEFORE GIMBAL)

$dCM/dCL : -0.133$

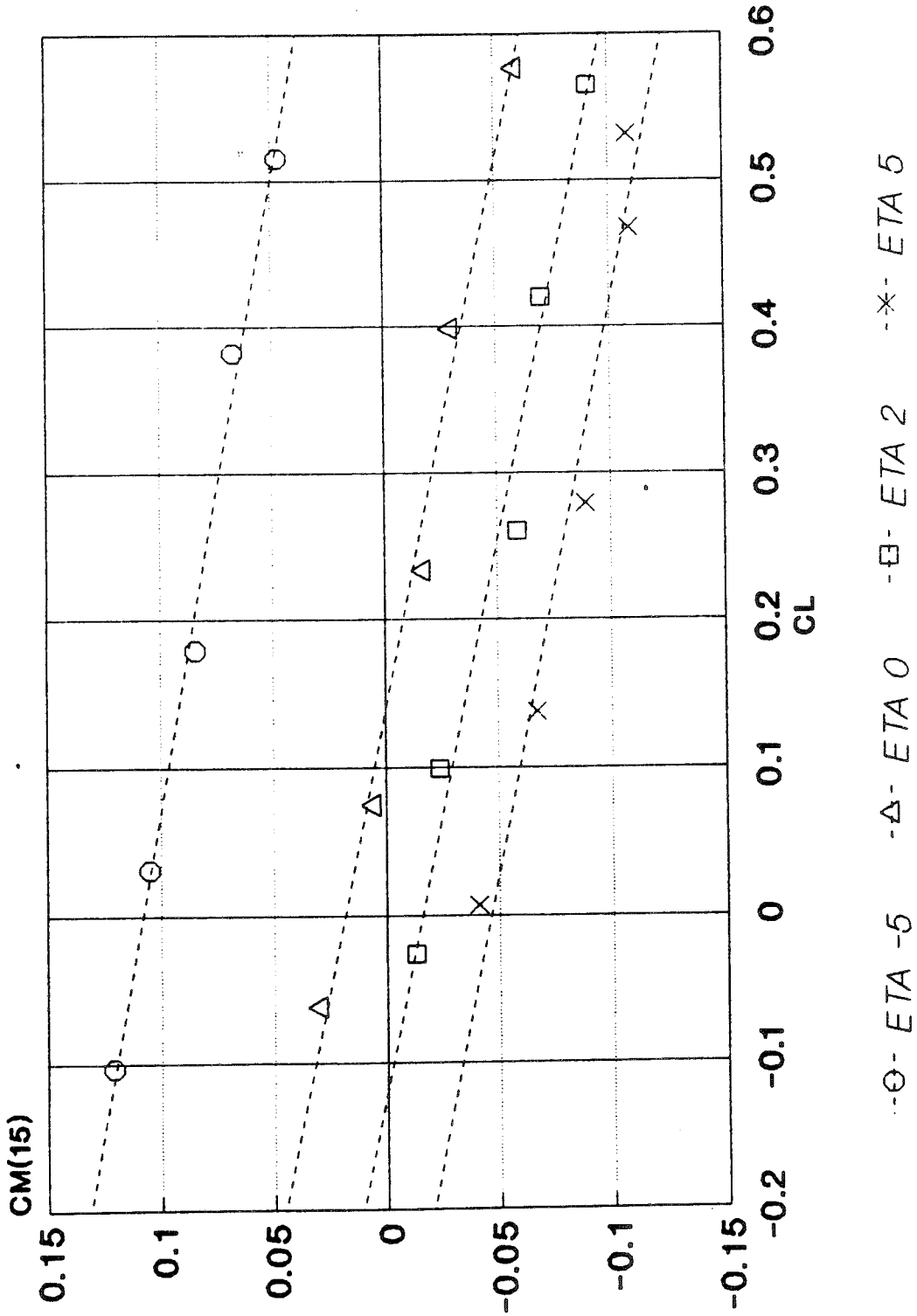


FIG. A-4: CM vs CL (15mm BEFORE GIMBAL)

APPENDIX B:

PITCH AND ROLL DECAY GRAPHS.

FIG. B-1: SPRING 1

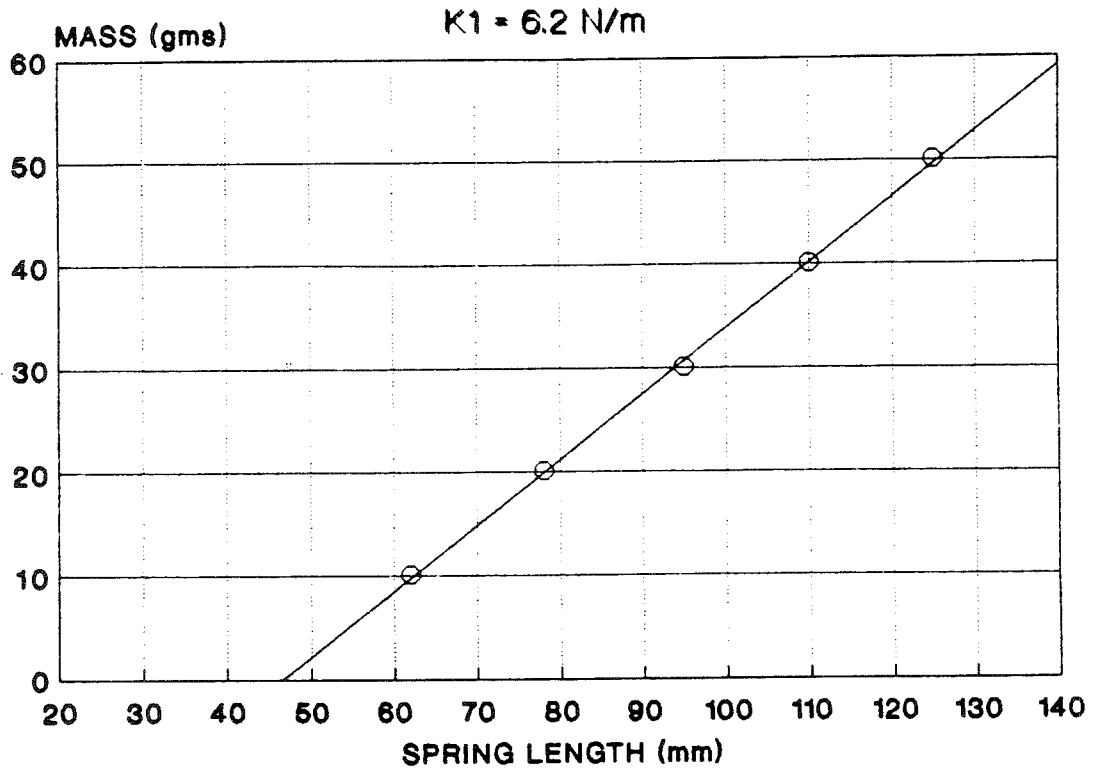


FIG. B-2: SPRING 2

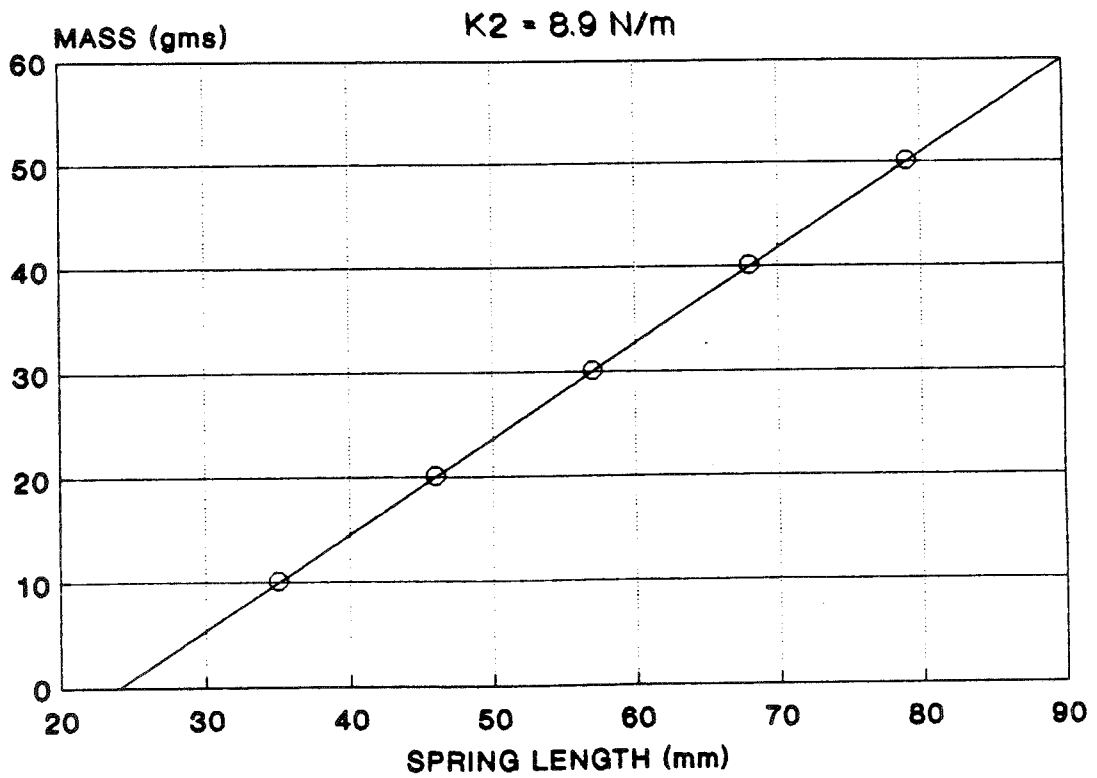


FIG. B-3: PITCH RESPONSE (K1 & K2).

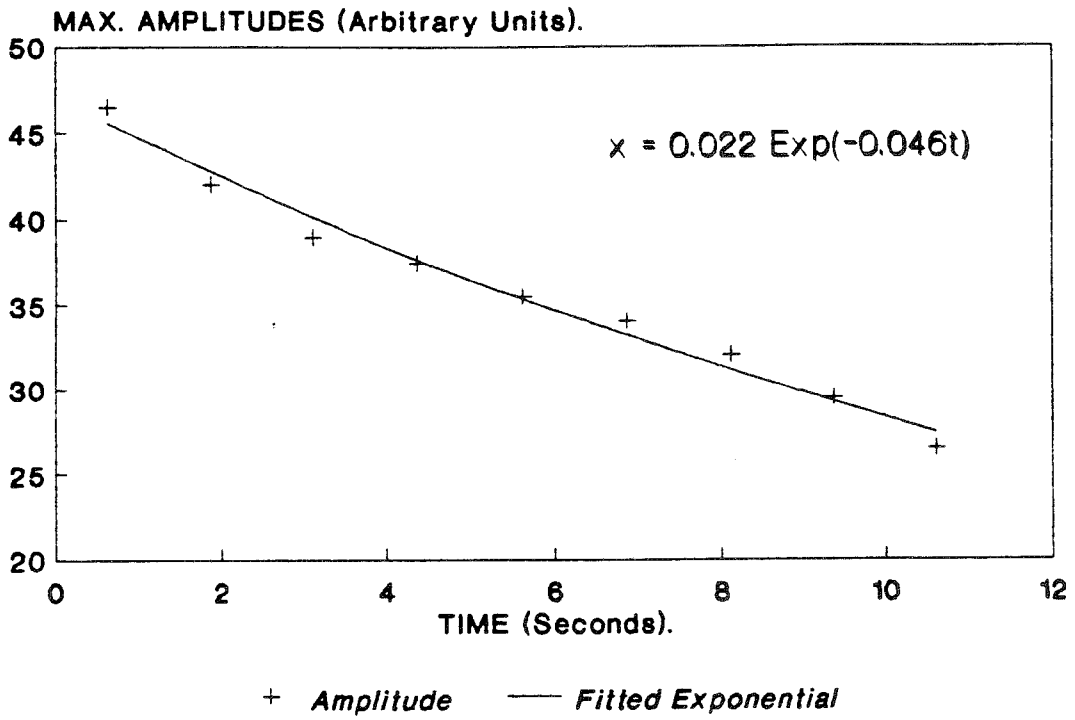
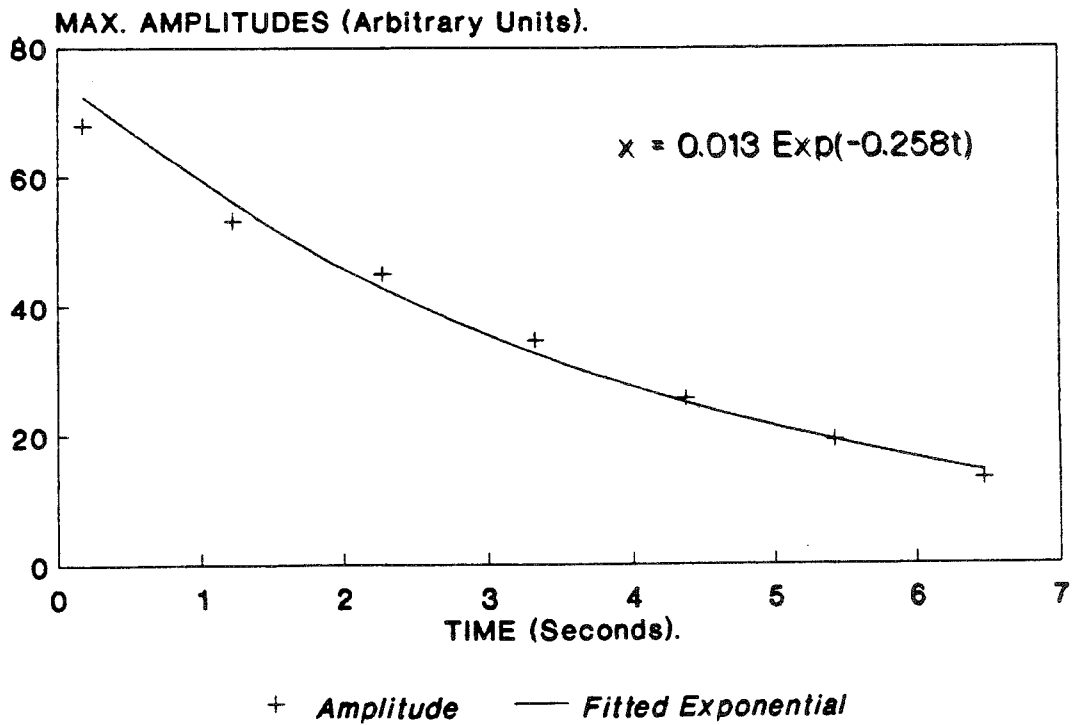


FIG. B-4: ROLL RESPONSE (K1 & K2)



APPENDIX C:

PROGRAM FOR DATA CONVERSION AND DIFFERENTIATION.


```

'*****
'*          DATA FORMAT CONVERSION PROGRAM          *
'*****

```

key off

```

dim chan(17)      'Channel numbers of input data files
dim y(17,5)       'Previous five data readings (for differentiation)
dim diff(17)      'Flags indicating whether to differentiate

```

```

vmax      =5      'Max 5 volts into 1401
channels=0      'Total number of channels being used
h         =1      'Time interval for differentiation

```

```

cls
screen 9
color 14,1
line (100,50)-(539,300),7,BF
locate 11,29: print "DATA FORMAT CONVERSION";
locate 12,37: print "PROGRAM"
locate 23,5: print "";
locate 24,10: print "";

```

```

do while inkey$=""      'Wait for a keypress
loop

```

```

'*****
'*          MAIN PROGRAM BEGINS HERE          *
'*****

```

```

gosub format          'Get data format spec
gosub filename        'Get converted data filename
gosub convert         'Convert data

```

```

cls
locate 2,30: print "Conversion complete:";
locate 4,30: print "Data held in ";f$;
locate 8,23: input "Do you want to run the program again";a$
if left$(a$,1)="Y" or left$(a$,1)="y" then run
locate 10,28: print "type SYSTEM to return to DOS";
shell "cd\tbasic"
end

```

'----- END OF MAIN PROGRAM -----'

```

'*****
'*          DATA FORMAT SPECIFICATION          *
'*****

```

```

format:
cls
locate 2,30
print "DATA FORMAT SETUP:"
locate 6,15
print "Please type in the channels you wish to use, ending the
list with 99:";
locate 9,15
print "Append a ',1' to diff. a channel, otherwise leave blank";
print: print

```

entchan:

input "Channel, differentiate";a,b

if a=99 then goto ofst

if a<1 or a>16 or a<>int(a) then

play "A"

locate 23,30

print "Illegal channel";

for i=1 to 2000

next

locate 23,30

print space\$(15);

locate 11+channels,1

goto entchan

end if

channels=channels+1

chan(channels)=a

if b=1 then diff(channels)=1

goto entchan

ofst:

locate 18,5

input"Voltage offset to be added to each reading";offset

locate 19,5

input "What is the generic filename (ie. filename.CHn) ? ",a\$
dfile\$=left\$(A\$,8)

return

```
'*****  
'* FILE SAVING ROUTINE *  
'*****
```

filename:

shell "cd\TBASIC\data"

entry:

locate 20,5

input"What is the file which the data will be stored in? ",f\$

a=len(f\$)

for i = 1 to a

a\$=right\$(f\$,(a+1-i))

a\$=left\$(a\$,1)

if a\$="." then

locate 22,20

print"Illegal file name: no <.> allowed as <.DAT> is assumed.";

goto entry

end if

next i

'Check name of file


```

do
  conv$=" "
  for i=1 to channels
    seek £(I+2),byte*2      'Find correct position in input file
    get$ £(I+2),2,a$       'and get next data byte

    if eof(3) then exit loop 'Exit loop if end of 1st channel data
                              '(assumes all file lengths the same
length)
    'Calculate voltage:

    msb=asc(left$(a$,1))    'this is the first byte loaded
    lsb=asc(right$(a$,1))  'this is the second byte loaded

    minus=msb and 128       'msb of byte set if negative word
    msb=msb and 127        'mask off sign bit

    num=lsb+msb*256        'calculate numerical value from 1401
    volts=num/32767*vmax+offset 'conv. to volts & add any offset
    if minus=128 then volts=-volts 'and correct for sign

    'Do differentiation:

    for j=2 to 5            'Shift most recent five data points
      y(i,j-1)=y(i,j)      'along a FIFO stack
    next j

    y(i,5)=volts           'and enter newest data point

    conv$=conv$+str$(y(i,3))+ " " 'format a row of channel data

    if diff(i)=1 then

      'Calculate differential over last five data pts
      vdiff= ( -y(i,5)+8*y(i,4)-8*y(i,2)+y(i,1) )/12*h

      if byte<4 then vdiff=0      'Initial calc/d diffs.

      conv$=conv$+str$(vdiff)+" " 'add in diff. to row of data

    end if

  next i

  if byte>1 then print £2,conv$   'Write row data to output file
  byte=byte+1                     'Increment byte count

loop                               'Until all input data used up

for j=4 to 5                       'Output last two rows of data
  conv$=" "

  for i=1 to channels
    conv$=conv$+str$(y(i,j))+ " "
    if diff(i)=1 then conv$=conv$+str$(0) 'Incomplete data for diff
  for last pts
  next i

```

```
    print £2,conv$  
next j  
locate 15,29: print " TRANSFER COMPLETE "  
close £2  
for i=1 to channels  
  close £(i+2)  
next i  
return
```

